

Anticancer activity of a *cis*-dichloridoplatinum(II) complex of a chelating nitrogen mustard: Insight to unusual guanine binding mode and low deactivation by glutathione

Subhendu Karmakar, Kallol Purkait, Saptarshi Chatterjee and Arindam Mukherjee†*

†Department of Chemical Sciences Indian Institute of Science Education and Research
Kolkata, Mohanpur Campus, Nadia-741246, West Bengal, India.

*Corresponding author. Fax: (+91)033-25873118; Tel: (+91)033-25873121; E-mail:

a.mukherjee@iiserkol.ac.in

Contents

Table S1 Crystal Data, data Collection and refinement parameters for complex 2	6
Fig. S1 ^1H NMR of L1 in D_2O , 400 MHz.	7
Fig. S2 ^{13}C NMR of L1 in D_2O , 125 MHz.	7
Fig. S3 ^1H NMR of L2.HCl in D_2O , 400 MHz.	8
Fig. S4 ^{13}C NMR of L2.HCl in D_2O , 125 MHz.	8
Fig. S5 ^1H NMR of 1 in $\text{DMSO-}d_6$, 500 MHz.	9
Fig. S6 ^{13}C NMR of 1 in $\text{DMSO-}d_6$, 125 MHz.	9
Fig. S7 ^{13}C DEPT-135 of 1 in $\text{DMSO-}d_6$, 125 MHz.	10
Fig. S8 HMQC of 1 in $\text{DMSO-}d_6$	10
Fig. S9 ^{195}Pt NMR of 1 in $\text{DMSO-}d_6$, 107.5 MHz.	11
Fig. S10 ^1H NMR of 2 in $\text{DMSO-}d_6$, 500 MHz.	11
Fig. S11 ^{13}C NMR of 2 in $\text{DMSO-}d_6$, 125 MHz.	12
Fig. S12 ^{13}C DEPT-135 of 2 in $\text{DMSO-}d_6$, 125 MHz.	12
Fig. S13 HMQC of 2 in $\text{DMSO-}d_6$	13
Fig. S14 ^{195}Pt NMR of 2 in $\text{DMSO-}d_6$, 107.5 MHz.	13
Fig. S15 Stack plot of aromatic region during the stability kinetics study of complex 1 in 20% PBS (pD 7.4, prepared in D_2O) – $\text{DMSO-}d_6$ mixture by ^1H NMR, where \blacklozenge & \bullet indicate the intact complex 1 & complex 1b and \blacktriangle & \blacktriangledown indicate the aquated complex 1a & 1c respectively.	14
Fig. S16 Stack plot of aromatic region during the binding kinetics study of 1 with 9-EtG (1:3) in 20% PBS (pD 7.4, prepared in D_2O) – $\text{DMSO-}d_6$ by ^1H NMR, where \blacklozenge & \bullet indicate the intact complex 1 & complex 1b and \blacktriangle & \blacktriangledown indicate the aquated complex 1a & 1c respectively. \blacksquare indicates the signals of 9-EtG bound complexes 1d & 1e . H8 of free 9-EtG is shifted downfield to H8* & H8** of 9-EtG bound complexes 1d & 1e respectively.	14
Fig. S17 Stack plot of binding kinetics study of 1 with 9-EtG (1:3) in 20% PBS (pD 7.4, prepared in D_2O) – $\text{DMSO-}d_6$ by ^{195}Pt NMR. The data taken after 2 h shows no binding of 9-EtG with 1 . After 24 h complex 1 signal at -2135.8 ppm diminished and two poorly resolvable signals of 9-EtG bound complexes 1d & 1e at -2203.0 & -2205.6 ppm respectively appear.	15
Table S2 Species found in ESI-MS during the stability/binding kinetics studies of 1 by ^1H NMR	15

Fig. S18 ESI-MS speciation recorded during monitoring of stability kinetics of the complex 1 by ^1H NMR after 3 h in 20% PBS (pD 7.4, prepared in D_2O) – $\text{DMSO}-d_6$ mixture.	18
Fig. S19 ESI-MS speciation recorded during monitoring of the 9-EtG binding kinetics with complex 1 by ^1H NMR after 1 d in 20% PBS (pD 7.4, prepared in D_2O) – $\text{DMSO}-d_6$ mixture.	18
Fig. S20 Observed and simulated isotopic pattern of [1b (Scheme 4) + H^+] found in ESI-MS.	19
Fig. S21 Observed and simulated isotopic pattern of [1c (Scheme 4) – $2\text{H}^+ + \text{Na}^+ + \text{K}^+$] found in ESI-MS.	20
Fig. S22 Observed and simulated isotopic pattern of [1d (Scheme 4)] found in ESI-MS. .	21
Fig. S23 Observed and simulated isotopic pattern of [1e (Scheme 4)] found in ESI-MS. .	22
Fig. S24 Stack plot of aromatic region during the stability kinetics study of complex 2 in 20% PBS (pD 7.4, prepared in D_2O) – $\text{DMSO}-d_6$ mixture by ^1H NMR, where *, # and † indicate the signals of intact complex 2 , hydrolyzed complex 2a and aziridinium ion 2b respectively.	23
Fig. S25 Stack plot of aromatic region during the stability kinetics study of complex 2 in 20% water – $\text{DMSO}-d_6$ mixture by ^1H NMR, where where *, # and † indicate the signals of intact complex 2 , hydrolyzed complex 2a and aziridinium ion 2b respectively.	23
Fig. S26 Stack plot of stability kinetics study of complex 2 in $\text{DMSO}-d_6$ by ^1H NMR.	24
Fig. S27 ^{195}Pt NMR of complex 2 in $\text{DMSO}-d_6$ after 8 h where peak at –2157.5 and –2973.6 ppm represent the chemical shift of 2 and DMSO bound complex 2 respectively.	24
Fig. S28 Stack plot of stability kinetics study of 2 (6 mM) in 40% DMEM- $\text{DMSO}-d_6$ by ^{195}Pt NMR. The peak at –2159.8 ppm is for intact complex 2 and peak at –2956.9 may signify S– bonded 2 . During experimentation some amount of the native complex precipitated.	25
Fig. S29 Stack plot of aliphatic region during the binding kinetics study of 2 with 9-EtG (1:3) in 20% PBS (pD 7.4, prepared in D_2O) – $\text{DMSO}-d_6$ by ^1H NMR, where * and ‡ indicate the signals of intact complex 2 and 9-EtG bound complexes 2d & 2e respectively. NH_2 of free 9-EtG is shifted upfield to NH_2' & NH_2'' of 9-EtG bound complexes 2d & 2e respectively. Me of free 9-EtG is shifted downfield to Me' & Me'' of 9-EtG bound complexes 2d & 2e respectively.	25
Fig. S30 Stack plot of binding kinetics study of 2 with 9-EtG (1:3) in 20% PBS (pD 7.4, prepared in D_2O) – $\text{DMSO}-d_6$ by ^{195}Pt NMR. The data taken after 2 h shows no binding of 9-EtG with 2 . After 24 h complex 2 signal at –2159.8 ppm diminished and two closely spaced signals of 9-EtG bound complexes 2d & 2e at –2216.0 & –2205.0 ppm respectively appear.	26
Fig. S31 Stack plot of aliphatic region during the binding kinetics study of 2 with GSH in 20% PBS (pD 7.4, prepared in D_2O) – $\text{DMSO}-d_6$ by ^1H NMR, where *, § and † indicate	

the signals of intact complex 2 , GSH bound complex 2c and aziridinium ion 2b respectively.	26
Fig. S32 Stack plot of aromatic region during the binding kinetics study of 2 with GSH in 20% PBS (pD 7.4, prepared in D ₂ O) – DMF- <i>d</i> ₇ by ¹ H NMR, where *, § and † indicate the signals of intact complex 2 , GSH bound complex 2c and aziridinium ion 2b respectively.	27
Fig. S33 Stack plot of binding kinetics study of 2 with GSH (1:3) in 20% PBS (pD 7.4, prepared in D ₂ O) – DMF- <i>d</i> ₇ by ¹⁹⁵ Pt NMR.. After 6 h complex signal GSH bound complex 2c at –2910.9 ppm appears along with initial signal of complex 2 at –2164.6 ppm. After a day the ¹⁹⁵ Pt signal of 2c vanishes with very small amount of unreacted complex 2 signal.	27
Fig. S34 Stack plot of IR spectra of 2 , GSH and yellow ppt found in the reaction of 2 with GSH (1:3) in 20% PBS (pD 7.4, prepared in D ₂ O) – DMF- <i>d</i> ₇ . A) Sharp band of C–Cl stretching frequency 772 cm ^{–1} of 2 vanished in yellow ppt. B) Carbonyl stretching band of GSH and yellow ppt. C) S–H stretching band at 2522 cm ^{–1} in GSH vanished in yellow ppt and a broad band at 3550–2700 cm ^{–1} for polymeric nature of yellow ppt.	28
Table S3 Species found in ESI-MS during the stability/binding kinetics studies of 2 by ¹ H NMR. The drawings of the respective species are given below the tabulated data	29
Fig. S35 ESI-MS speciation recorded during monitoring of stability kinetics of the complex 2 by ¹ H NMR after 1 d in 20% PBS (pD 7.4, prepared in D ₂ O) – DMSO- <i>d</i> ₆ mixture.	31
Fig. S36 ESI-MS speciation recorded during monitoring of stability kinetics of the complex 2 by ¹ H NMR after 3 d in 20% water – DMSO- <i>d</i> ₆ mixture.....	32
Fig. S37 ESI-MS speciation recorded during monitoring of the 9-EtG binding kinetics with complex 2 by ¹ H NMR after 2 d in 20% PBS (pD 7.4, prepared in D ₂ O) – DMSO- <i>d</i> ₆ mixture.	32
Fig. S38 ESI-MS speciation recorded during monitoring of the GSH binding kinetics with complex 2 by ¹ H NMR after 2 h in 20% PBS (pD 7.4, prepared in D ₂ O) – DMSO- <i>d</i> ₆ mixture.	33
.....	33
Fig. S39 ESI-MS speciation recorded during monitoring of the GSH binding kinetics with complex 2 by ¹ H NMR after 1 d in 20% PBS (pD 7.4, prepared in D ₂ O) – DMSO- <i>d</i> ₆ mixture.	33
Fig. S40 Observed and simulated isotopic pattern of [2a (Scheme 5) – 2H ⁺ + Na ⁺ + K ⁺] found in ESI-MS.	34
Fig. S41 Observed and simulated isotopic pattern of [2b (Scheme 5)] found in ESI-MS. .	35
Fig. S42 Observed and simulated isotopic pattern of [2c (Scheme 5)] found in ESI-MS. .	36
Fig. S43 Observed and simulated isotopic pattern of [2d (Scheme 5)] found in ESI-MS. .	37
Fig. S44 Observed and simulated isotopic pattern of [2e (Scheme 5)] found in ESI-MS. .	38

Fig. S45 Plots of cell viability (%) vs. log of μM concentrations of 1 against A) MCF-7 and B) HeLa WT cell lines after incubation for 48 h determined from MTT assays under normoxic condition. The plots provided are for one independent experiment out of the three independent experiments.....	39
Fig. S46 Plots of cell viability (%) vs. log of μM concentrations of 2 against A) MCF-7, B) A549, C) HeLa WT, D) MIA PaCa2 and E) HEK293 cell lines after incubation for 48 h determined from MTT assays under normoxic condition. The plots provided are for one independent experiment out of the three independent experiments.	39
Fig. S47 Plots of cell viability (%) vs. log of μM concentrations of 2 against A) MCF-7 and B) A549 cell lines after incubation for 48 h determined from MTT assays under normoxic condition in presence of 250 μM and 400 μM GSH respectively. The plots provided are for one independent experiment out of the three independent experiments.	39
Fig. S48 Plots of cell viability (%) vs. log of μM concentrations of 2 against A) MCF-7 and B) A549 cell lines after incubation for 48 h determined from MTT assays under hypoxic condition. The plots provided are for one independent experiment out of the three independent experiments.	40
Fig. S49 Plots of cell viability (%) vs. log of μM concentrations of 2 against A) MCF-7 and B) A549 cell lines after incubation for 48 h determined from MTT assays under hypoxic condition in presence of 250 μM and 400 μM GSH respectively. The plots provided are for one independent experiment out of the three independent experiments.	40
Fig. S50 Plots of cell viability (%) vs. log of μM concentrations of 2 against A) MIA PaCa2 cell line after incubation for 48 h determine from MTT assays under hypoxic condition and B) MIA PaCa2 cell lines after incubation for 48 h under hypoxic condition in presence of 100 μM GSH determined from MTT assays. The plots provided are for one independent experiment out of the three independent experiments.	40
Fig. S51 Cell cycle arrest of MCF-7 treated with 2 for 24 h. (A) DMSO control, (B) 6 μM , (C) 8 μM and D) 10 μM of 2 treated cells. The figure represents one independent experiment.....	41
Fig. S52 Cell cycle arrest of MCF-7 treated with cisplatin for 24 h. (A) DMSO control, (B) 2 μM , (C) 4 μM and D) 6 μM of cisplatin treated cells. The figure represents one independent experiment.	41
Fig. S53 Cell cycle arrest of MIA PaCa2 treated with 2 and cisplatin respectively for 24 h. (A) DMSO control, (B) 2.5 μM , (C) 3.5 μM and D) 4.5 μM of 2 and 15 μM of cisplatin treated cells. The figure represents one independent experiment.	41
Table S4 Cell cycle analysis of MCF-7 cells treated with 2 ^a	42
Table S5 Cell cycle analysis of MCF-7 cells treated with cisplatin ^a	42
Table S6 Cell cycle analysis of MIA PaCa2 cells treated with 2 and cisplatin ^a	42

Table S1 Crystal Data, data Collection and refinement parameters for complex **2**

2	
Empirical formula	C ₁₀ H ₁₄ Cl ₄ N ₂ Pt
Formula weight	499.12
Temperature (K)	100.01(10)
Wavelength (Å)	0.7107
Crystal system, space group	Monoclinic <i>P</i> 2 ₁ / <i>c</i>
<i>a</i> (Å)	8.5829(11)
<i>b</i> (Å)	10.4134(11)
<i>c</i> (Å)	15.2859(16)
α (deg.)	90.00
β (deg.)	98.85(10)
γ (deg.)	90.00
Volume (Å ³)	1350.0(3)
<i>Z</i> , Calculated density (mg/mm ³)	4, 2.456
<i>F</i> (000)	936.0
μ /mm ⁻¹	11.163
Max. and min. transmission	0.518 and 1.000
Goodness-of-fit on <i>F</i> ²	1.008
Final <i>R</i> indices [<i>I</i> > 2σ(<i>I</i>)]	^a <i>R</i> ₁ = 0.0326, ^b <i>wR</i> ₂ = 0.0665
<i>R</i> indices (all data)	^a <i>R</i> ₁ = 0.0391, ^b <i>wR</i> ₂ = 0.0712

$$^a R_1 = \Sigma |F_o| - |F_c| / \Sigma |F_o|, \quad ^b wR_2 = [\Sigma [w(F_o^2 - F_c^2)^2] / \Sigma w(F_o^2)^2]^{1/2}$$

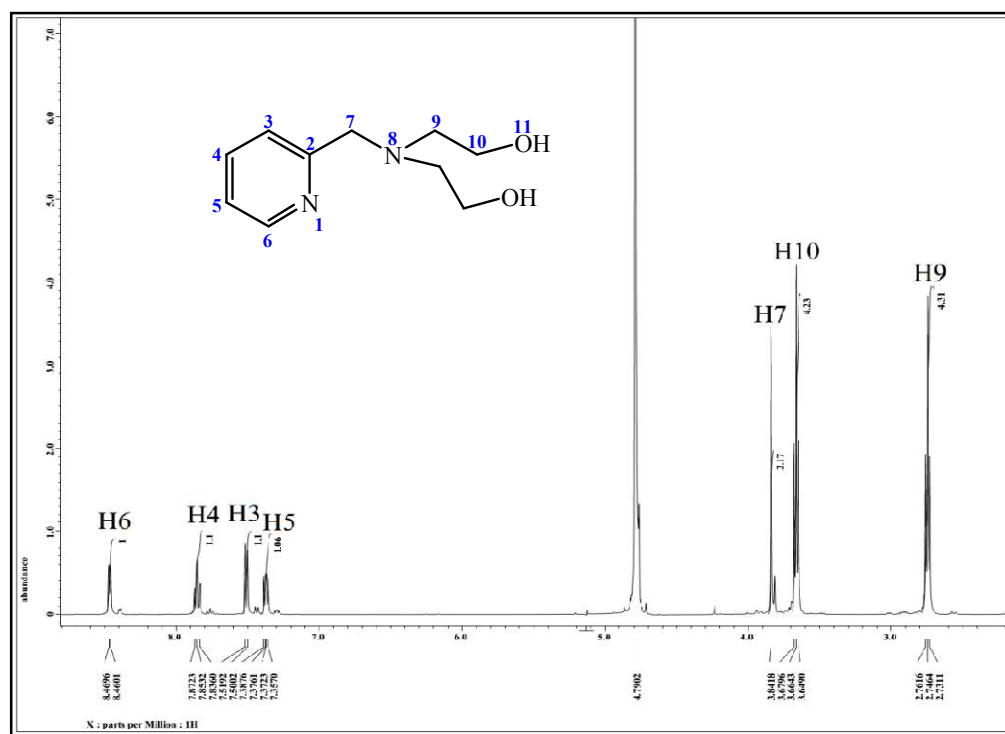


Fig. S1 ^1H NMR of L1 in D_2O , 400 MHz.

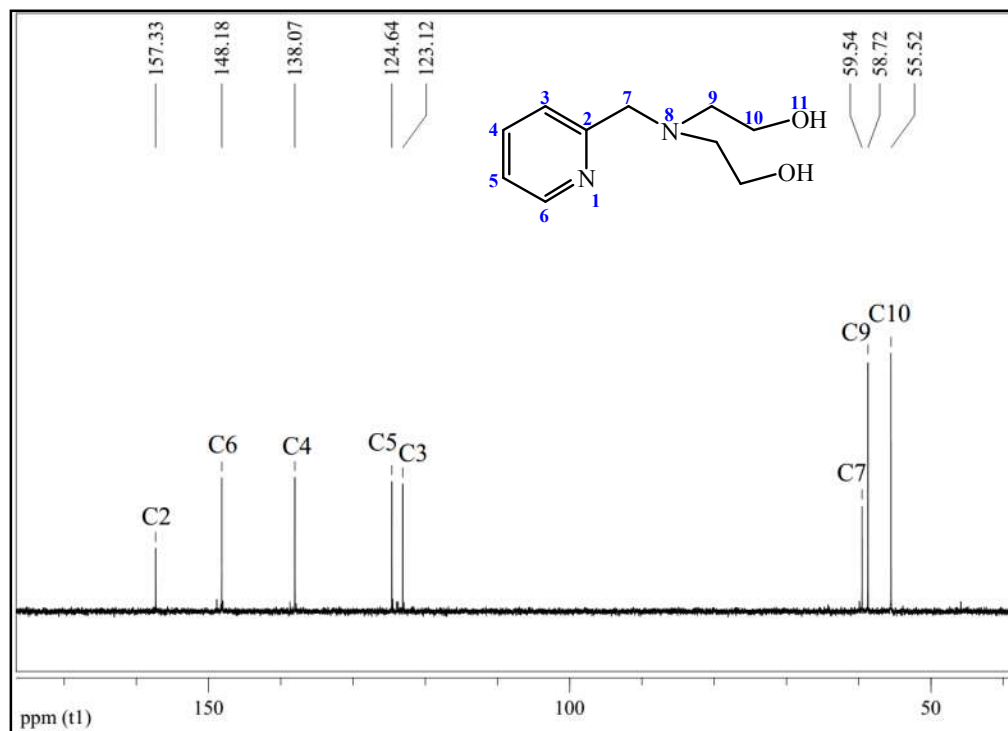


Fig. S2 ^{13}C NMR of L1 in D_2O , 125 MHz.

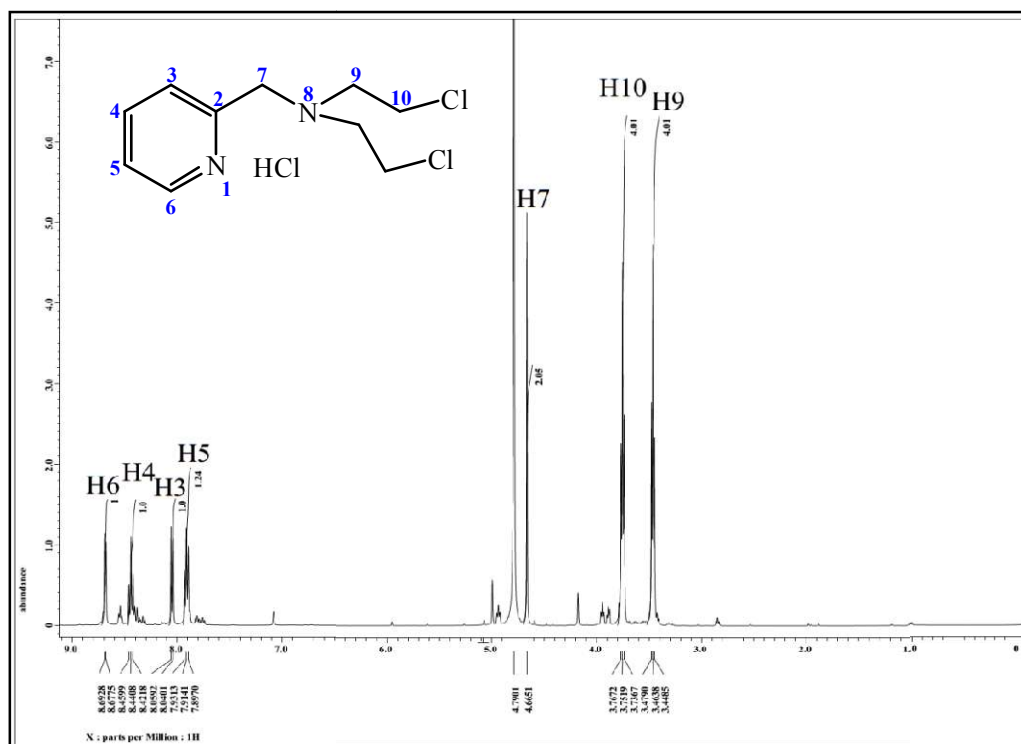


Fig. S3 ¹H NMR of L2.HCl in D₂O, 400 MHz.

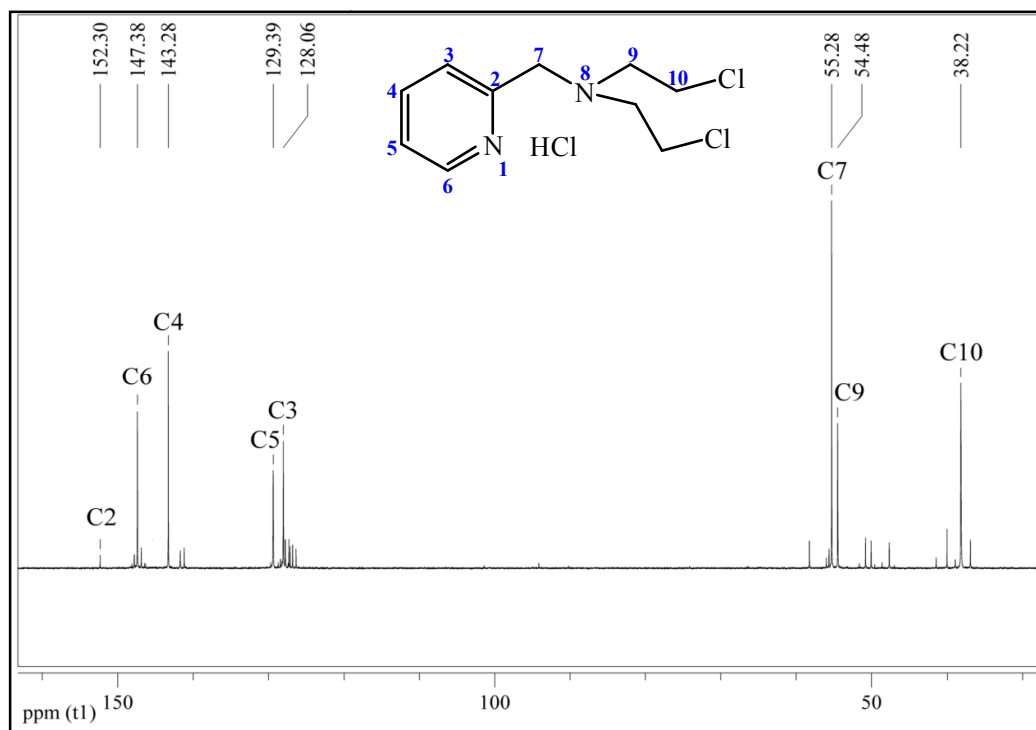


Fig. S4 ¹³C NMR of L2.HCl in D₂O, 125 MHz.

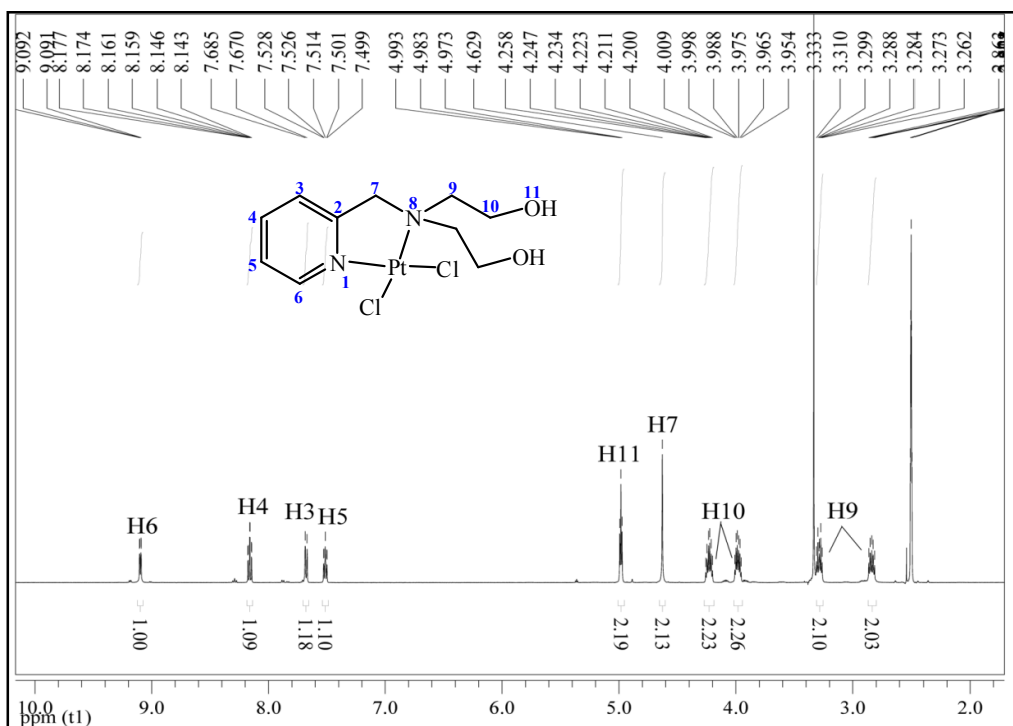


Fig. S5 ^1H NMR of **1** in $\text{DMSO-}d_6$, 500 MHz.

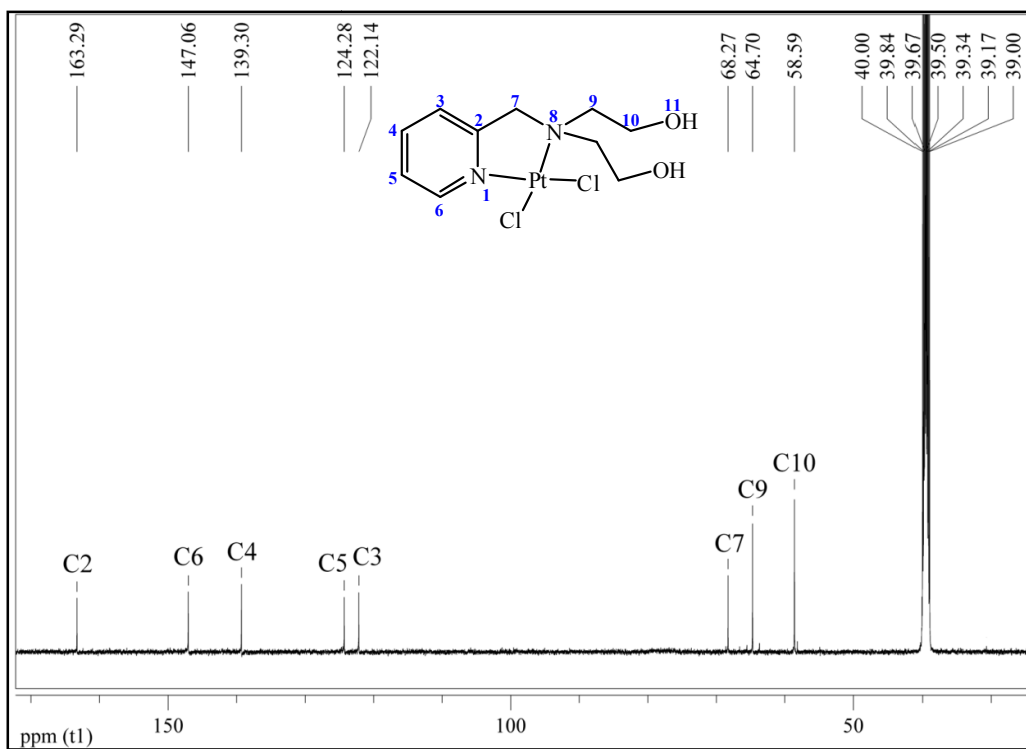


Fig. S6 ^{13}C NMR of **1** in $\text{DMSO-}d_6$, 125 MHz.

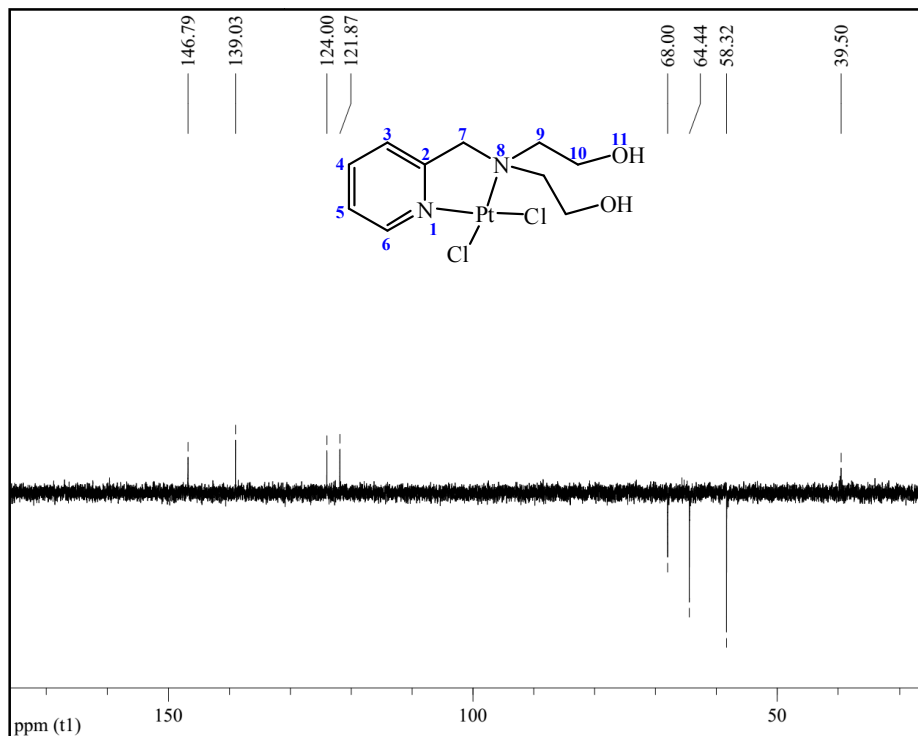


Fig. S7 ¹³C DEPT-135 of **1** in DMSO-*d*₆, 125 MHz.

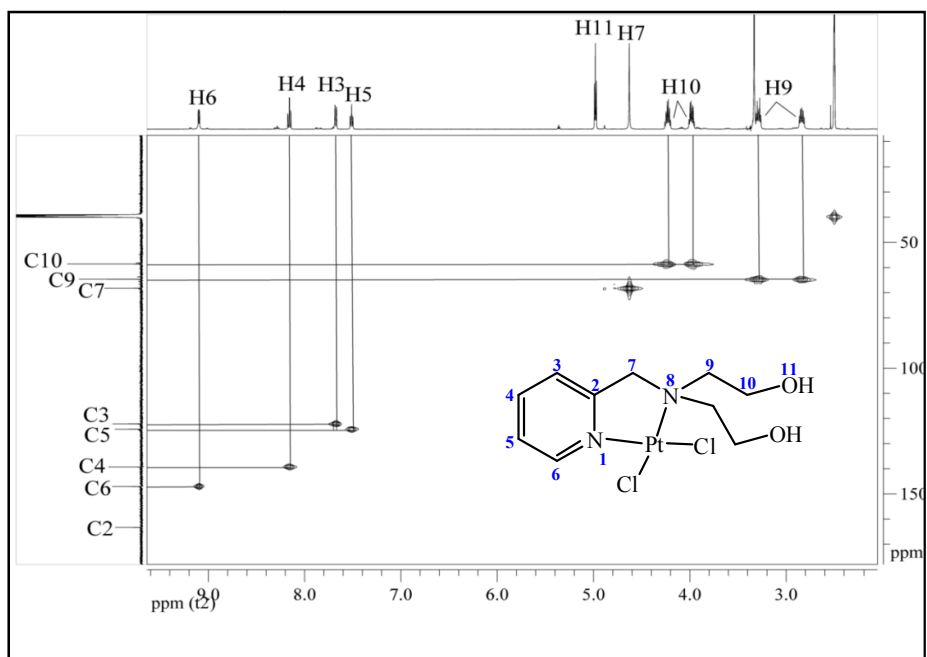


Fig. S8 HMQC of **1** in DMSO-*d*₆.

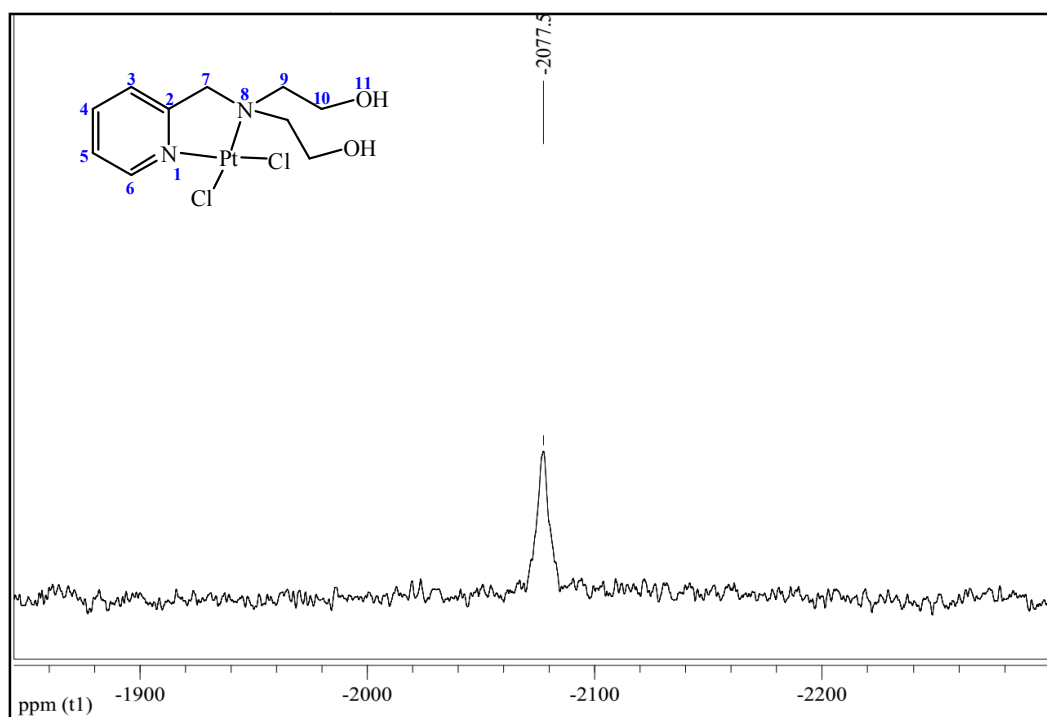


Fig. S9 ^{195}Pt NMR of **1** in $\text{DMSO-}d_6$, 107.5 MHz.

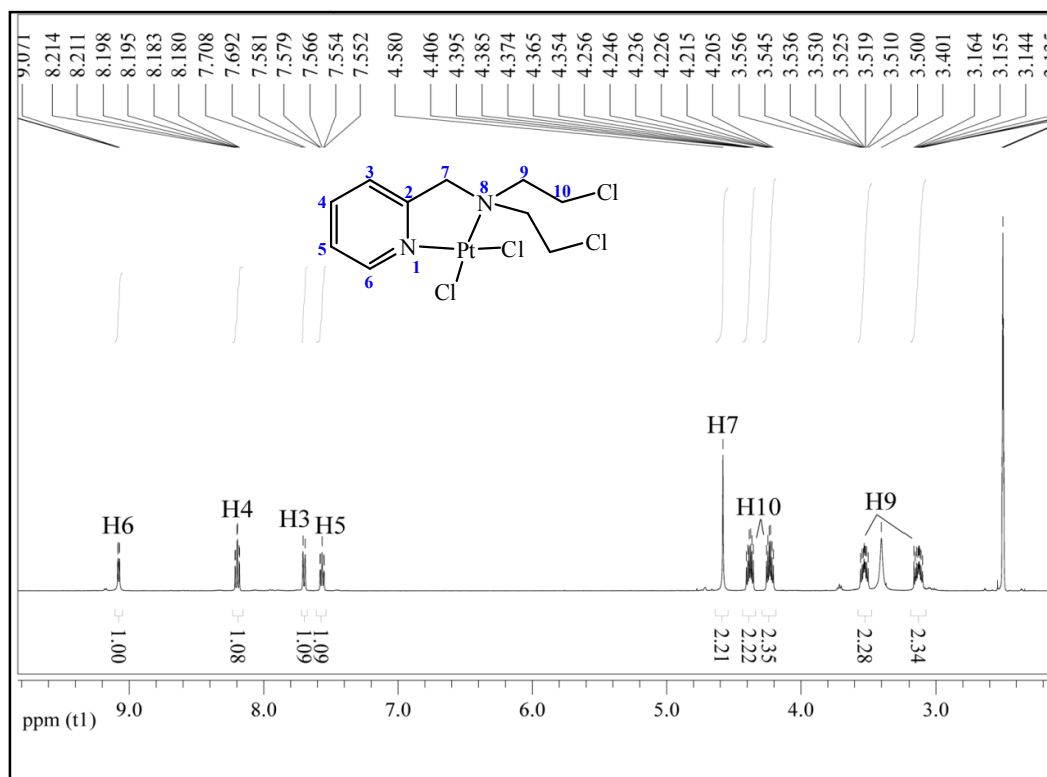


Fig. S10 ^1H NMR of **2** in $\text{DMSO-}d_6$, 500 MHz.

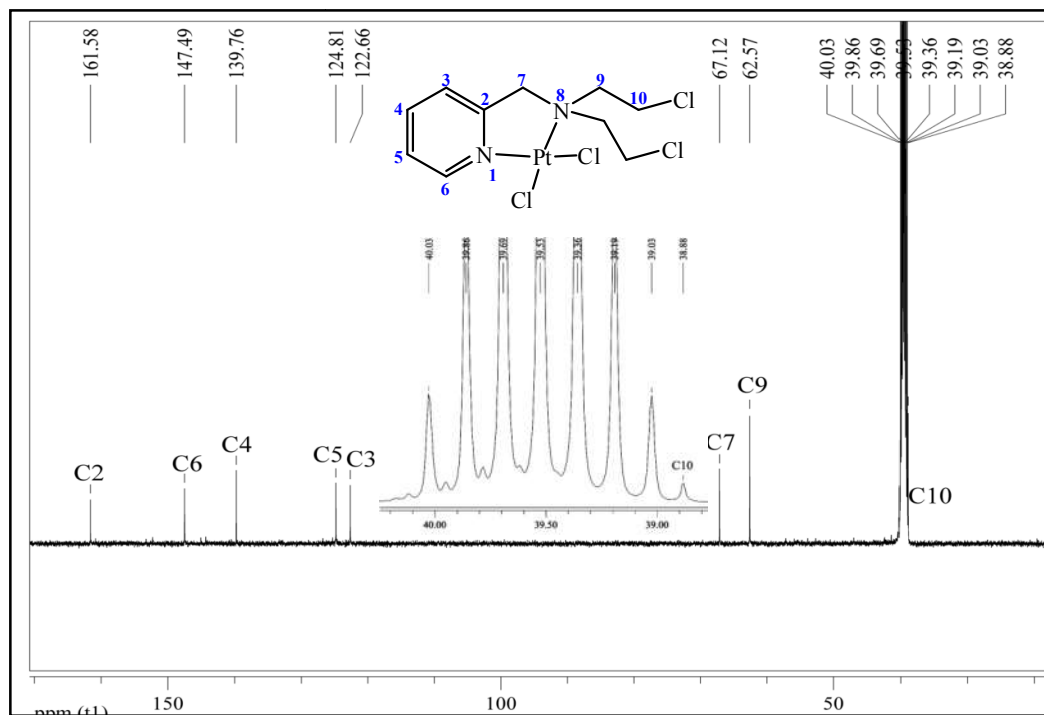


Fig. S11 ¹³C NMR of **2** in DMSO-*d*₆, 125 MHz.

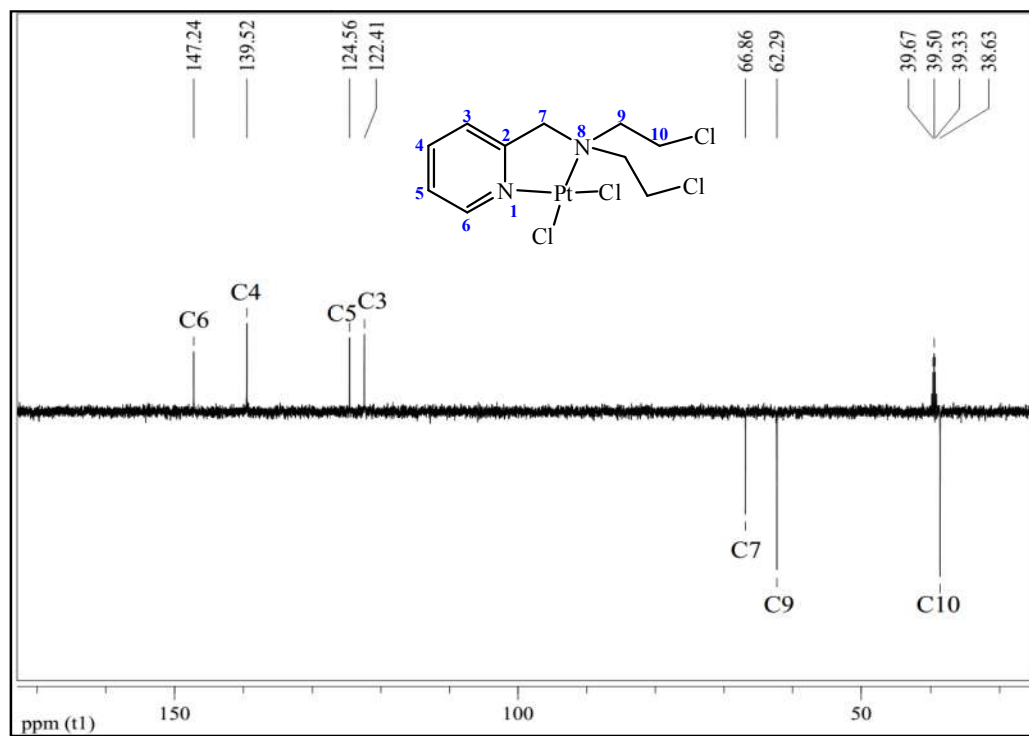


Fig. S12 ¹³C DEPT-135 of **2** in DMSO-*d*₆, 125 MHz.

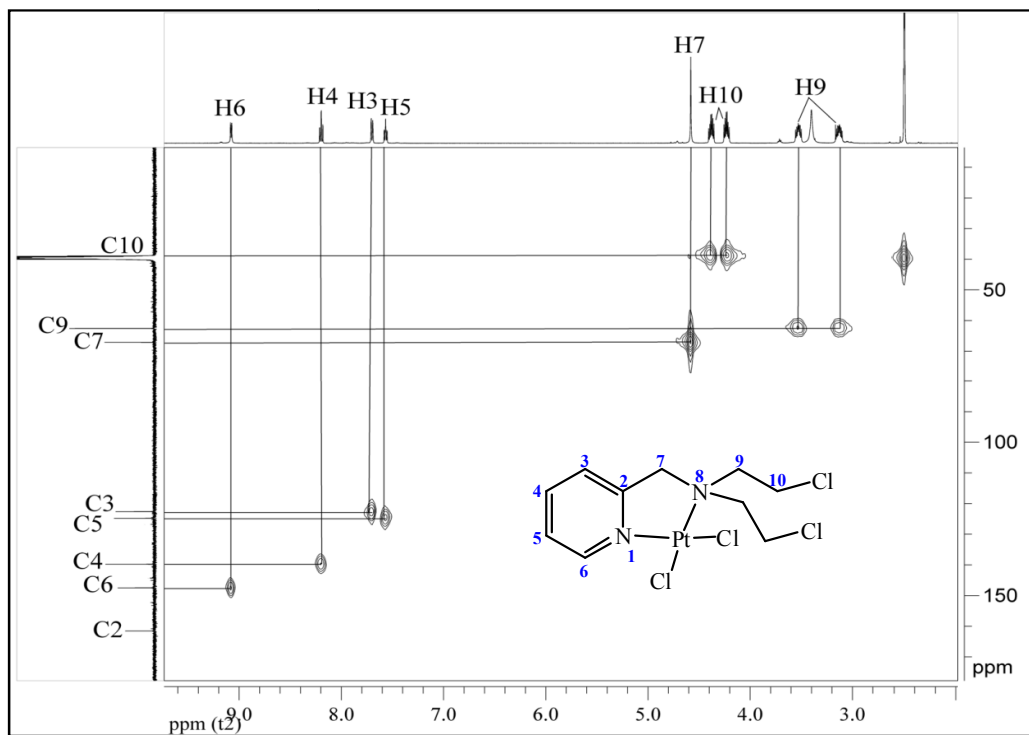


Fig. S13 HMQC of **2** in DMSO- d_6 .

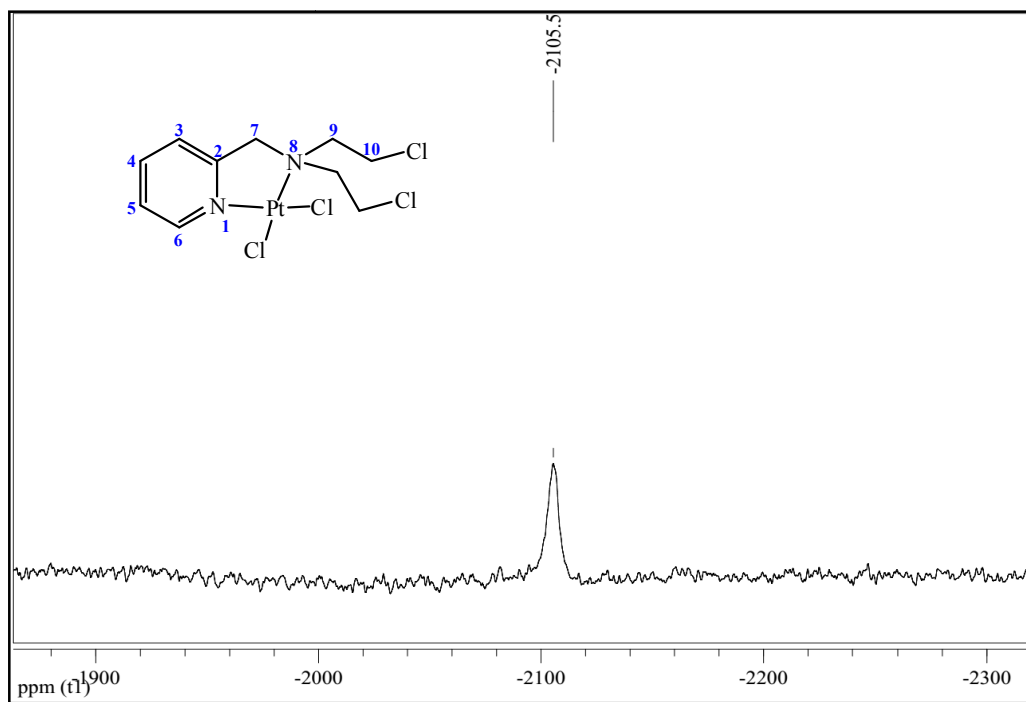


Fig. S14 ^{195}Pt NMR of **2** in DMSO- d_6 , 107.5 MHz.

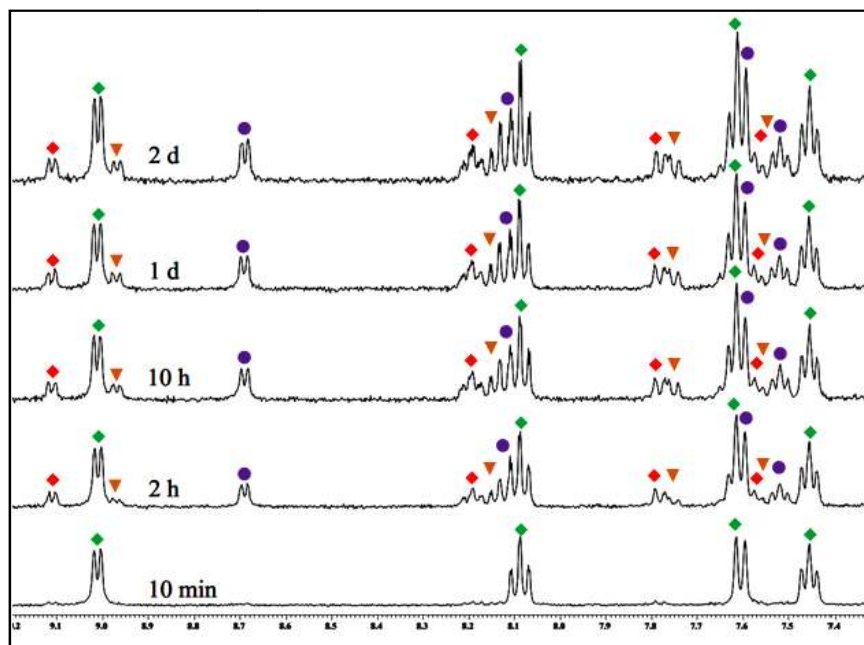


Fig. S15 Stack plot of aromatic region during the stability kinetics study of complex **1** in 20% PBS (pD 7.4, prepared in D₂O) – DMSO-*d*₆ mixture by ¹H NMR, where ♦ & ● indicate the intact complex **1** & complex **1b** and ▲ & ▼ indicate the aquated complex **1a** & **1c** respectively.

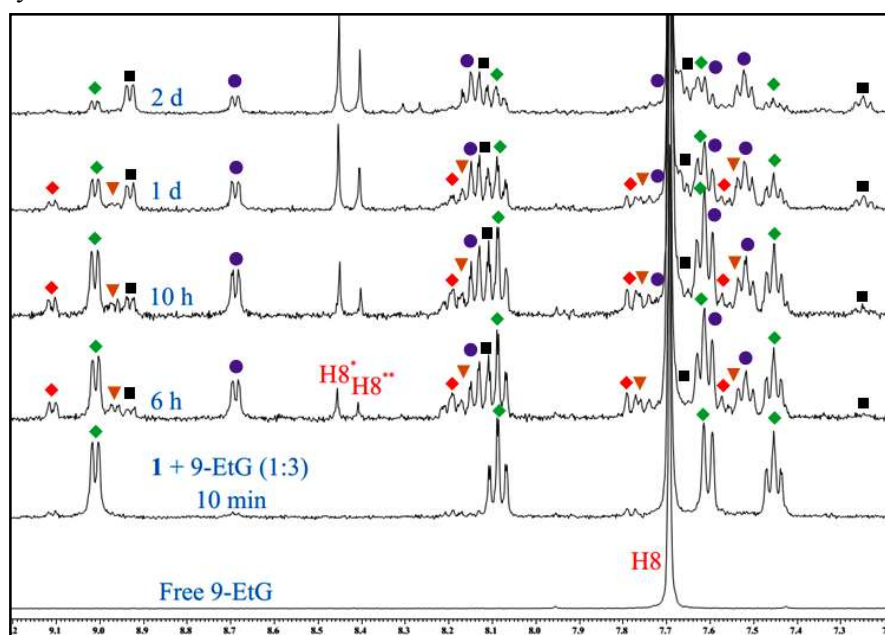


Fig. S16 Stack plot of aromatic region during the binding kinetics study of **1** with 9-EtG (1:3) in 20% PBS (pD 7.4, prepared in D₂O) – DMSO-*d*₆ by ¹H NMR, where ♦ & ● indicate the intact complex **1** & complex **1b** and ▲ & ▼ indicate the aquated complex **1a** & **1c** respectively. ■ indicates the signals of 9-EtG bound complexes **1d** & **1e**. H8 of free 9-EtG is shifted downfield to H8* & H8** of 9-EtG bound complexes **1d** & **1e** respectively.

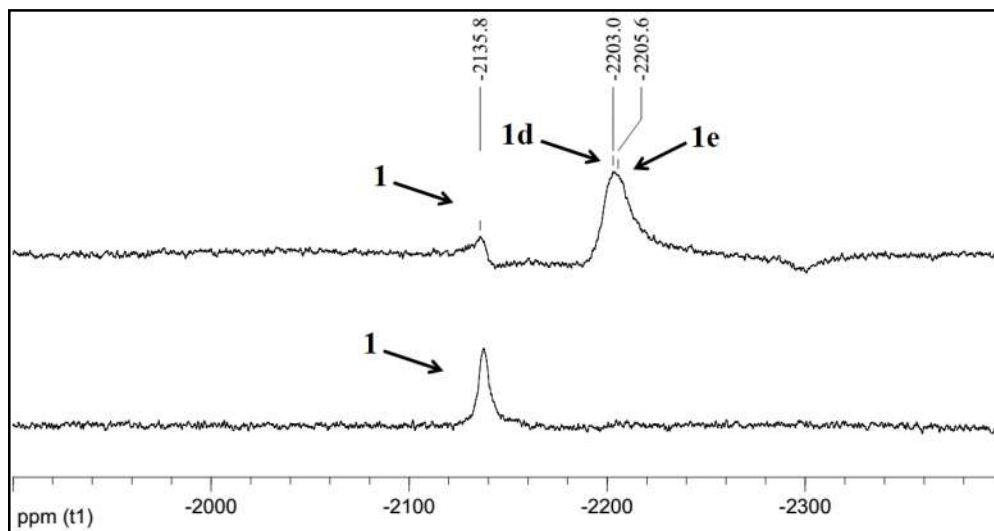


Fig. S17 Stack plot of binding kinetics study of **1** with 9-EtG (1:3) in 20% PBS (pD 7.4, prepared in D₂O) – DMSO-*d*₆ by ¹⁹⁵Pt NMR. The data taken after 2 h shows no binding of 9-EtG with **1**. After 24 h complex **1** signal at –2135.8 ppm diminished and two poorly resolvable signals of 9-EtG bound complexes **1d** & **1e** at –2203.0 & –2205.6 ppm respectively appear.

Table S2 Species found in ESI-MS during the stability/binding kinetics studies of **1** by ¹H NMR

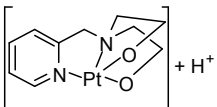
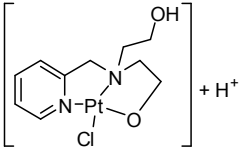
Species no.	Drawings	m/z_{calc}	Experiments	
			1 in 20% PBS (pD 7.4, prepared in D ₂ O) – DMSO- d_6	1 + 9-EtG (1:3) in 20% PBS (pD 7.4, prepared in D ₂ O) – DMSO- d_6
			m/z_{obs}	
I-a		390.0782	390.0811	390.0747
I-b		427.0539	427.0484	427.0508

Table S2 contd.

Table S2 Species found in ESI-MS during the stability/binding kinetics studies of **1** by ^1H NMR

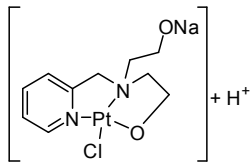
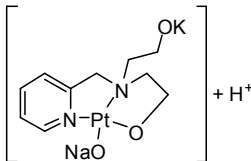
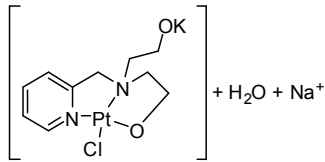
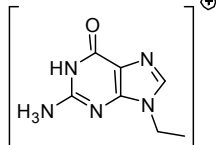
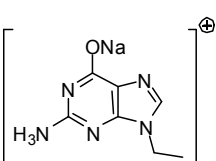
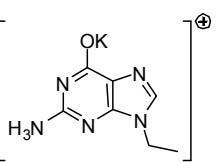
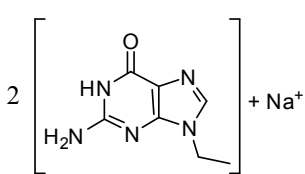
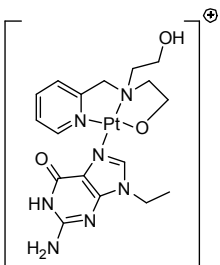
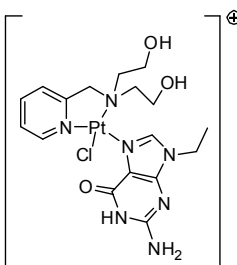
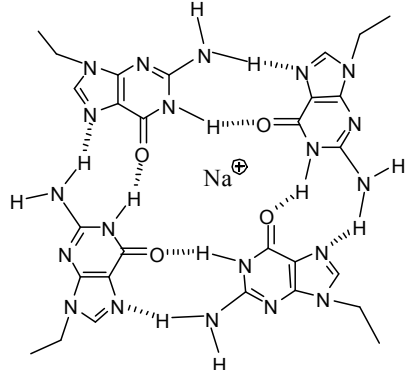
Species no.	Drawings	m/z_{calc}	Experiments	
			1 in 20% PBS (pD 7.4, prepared in D ₂ O) – DMSO- d_6	1 + 9-EtG (1:3) in 20% PBS (pD 7.4, prepared in D ₂ O) – DMSO- d_6
			m/z_{obs}	
I-c		449.0359	449.0396	449.0314
I-d		468.0266	468.0757	468.0773
I-e		505.0022	505.0659	505.0778
I-f		180.0885	-	180.0867
I-g		202.0705	-	202.0697
I-h		218.0444	-	218.0405
I-i		381.1512	-	381.1513

Table S2 contd.

Table S2 Species found in ESI-MS during the stability/binding kinetics studies of **1** by ^1H NMR

Species no.	Drawings	m/z_{calc}	Experiments	
			1 in 20% PBS (pD 7.4, prepared in D ₂ O) – DMSO- <i>d</i> ₆	1 + 9-EtG (1:3) in 20% PBS (pD 7.4, prepared in D ₂ O) – DMSO- <i>d</i> ₆
			m/z_{obs}	
I-j		569.1589	-	569.1595
I-k		606.1349	-	606.1368
I-l		739.3126	-	739.3171

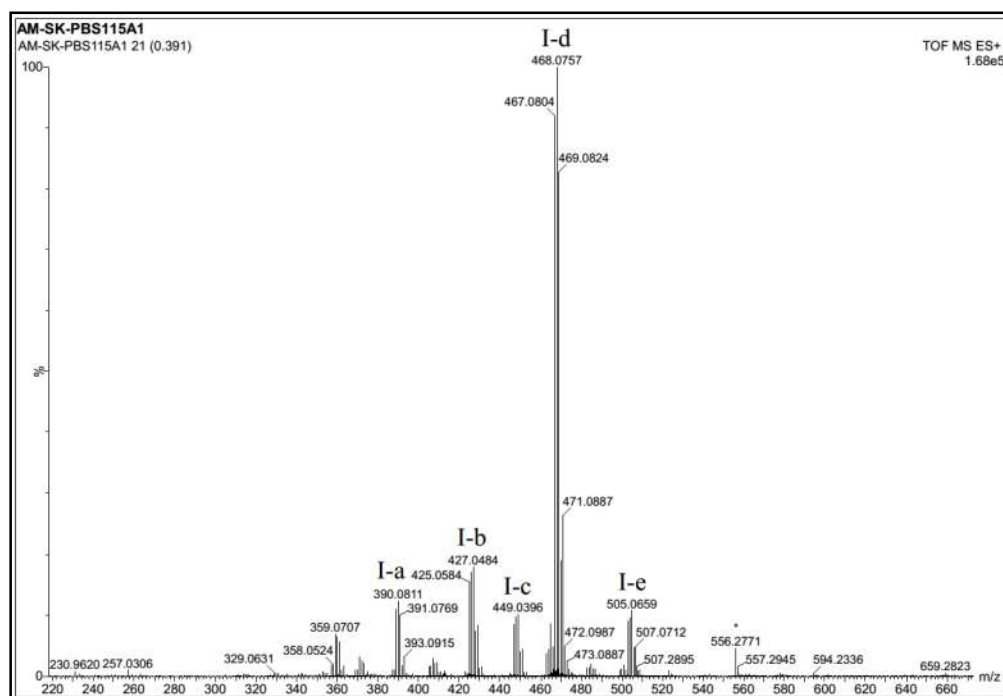


Fig. S18 ESI-MS speciation recorded during monitoring of stability kinetics of the complex **1** by ^1H NMR after 3 h in 20% PBS (pD 7.4, prepared in D_2O) – $\text{DMSO-}d_6$ mixture.

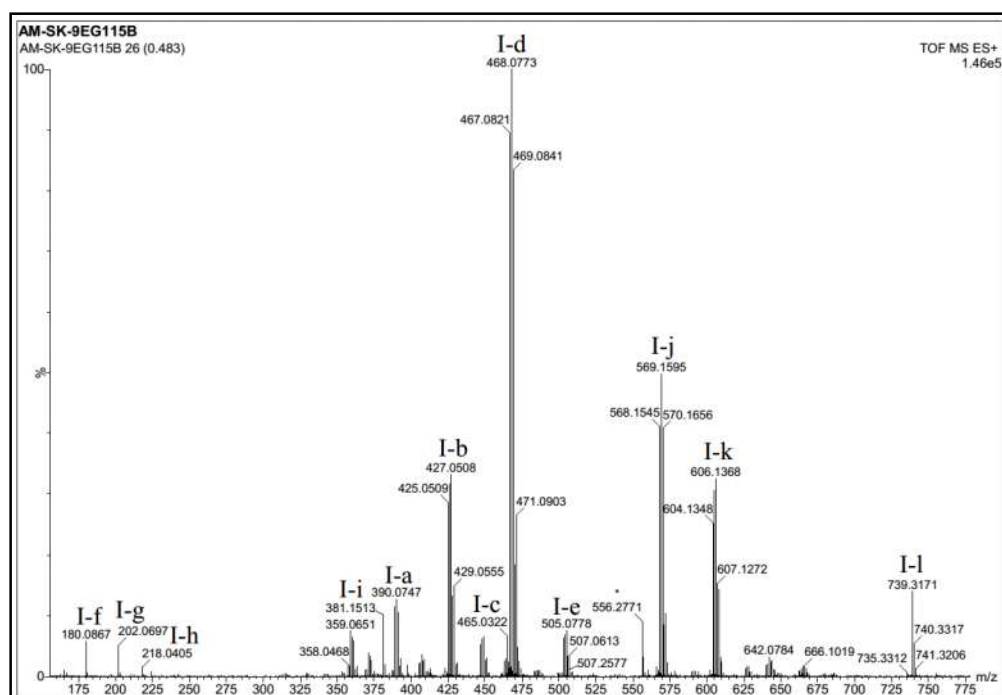


Fig. S19 ESI-MS speciation recorded during monitoring of the 9-EtG binding kinetics with complex **1** by ^1H NMR after 1 d in 20% PBS (pD 7.4, prepared in D_2O) – $\text{DMSO-}d_6$ mixture.

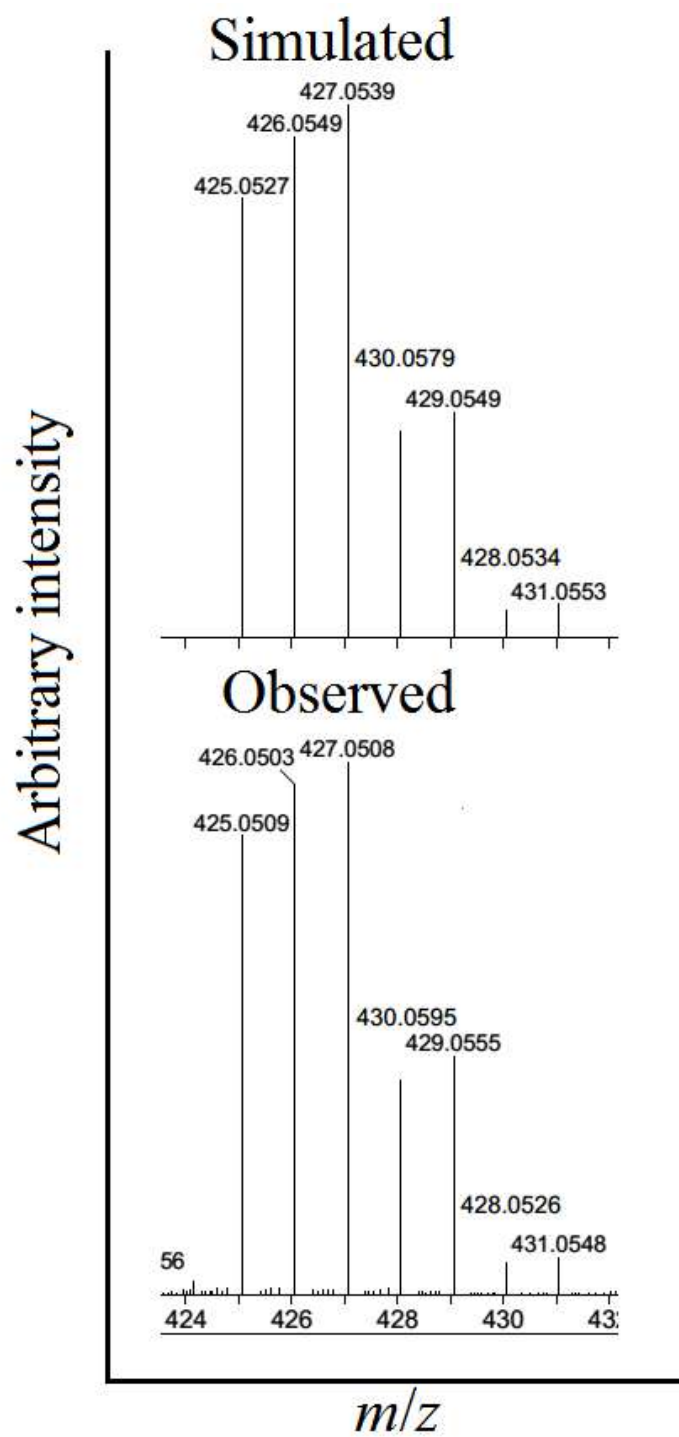


Fig. S20 Observed and simulated isotopic pattern of [**1b** (Scheme 4) + H⁺] found in ESI-MS.

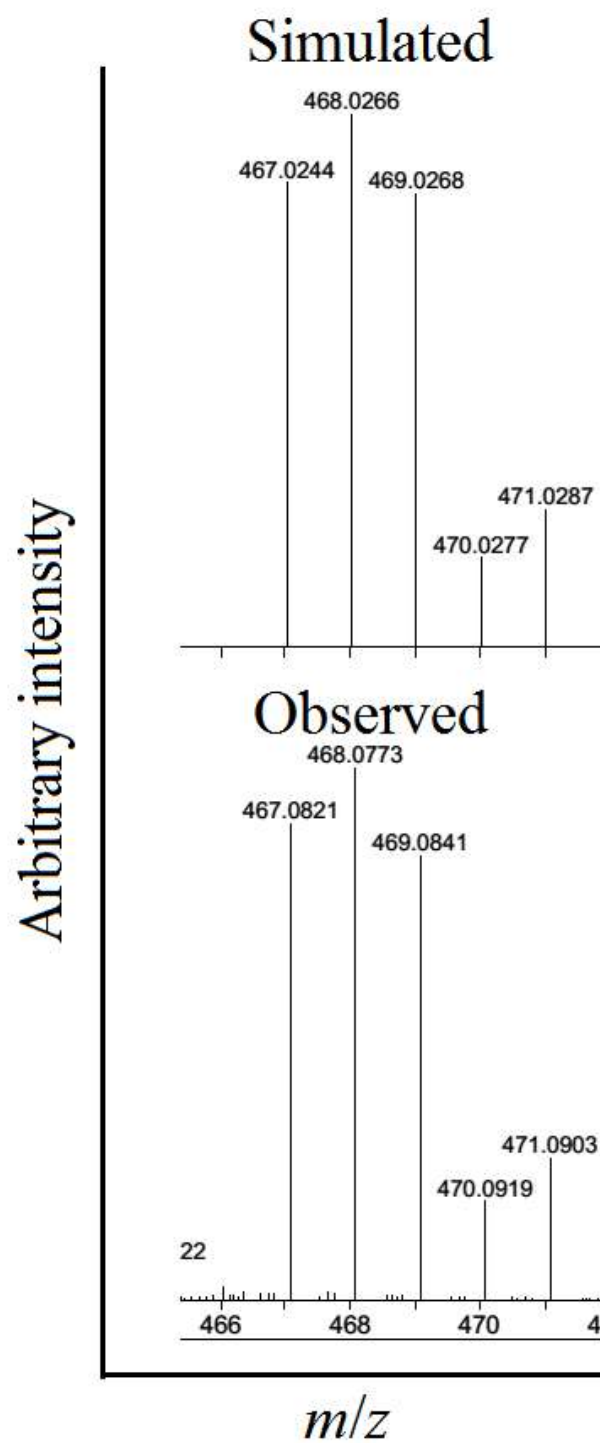


Fig. S21 Observed and simulated isotopic pattern of $[1\mathbf{c} \text{ (Scheme 4)} - 2\text{H}^+ + \text{Na}^+ + \text{K}^+]$ found in ESI-MS.

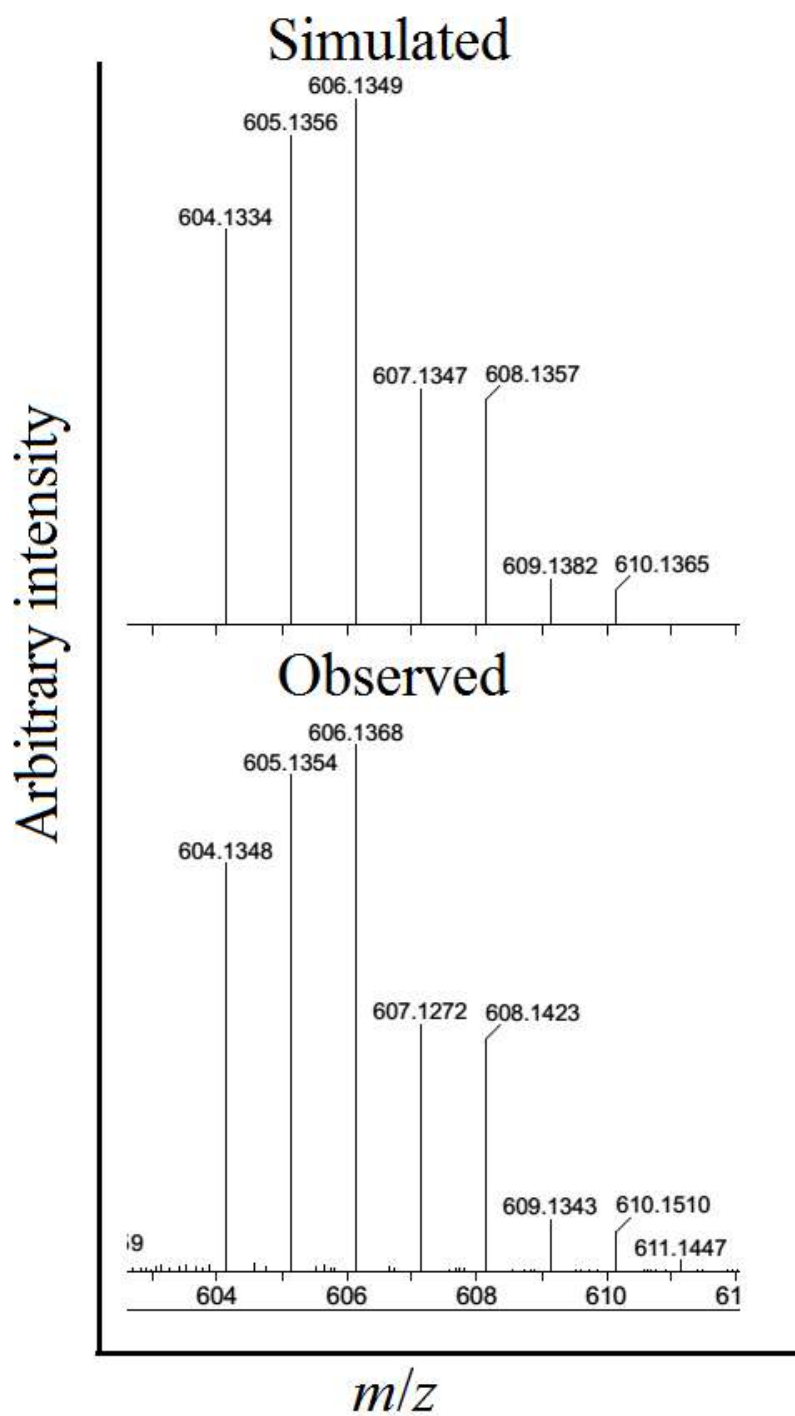


Fig. S22 Observed and simulated isotopic pattern of [**1d** (Scheme 4)] found in ESI-MS.

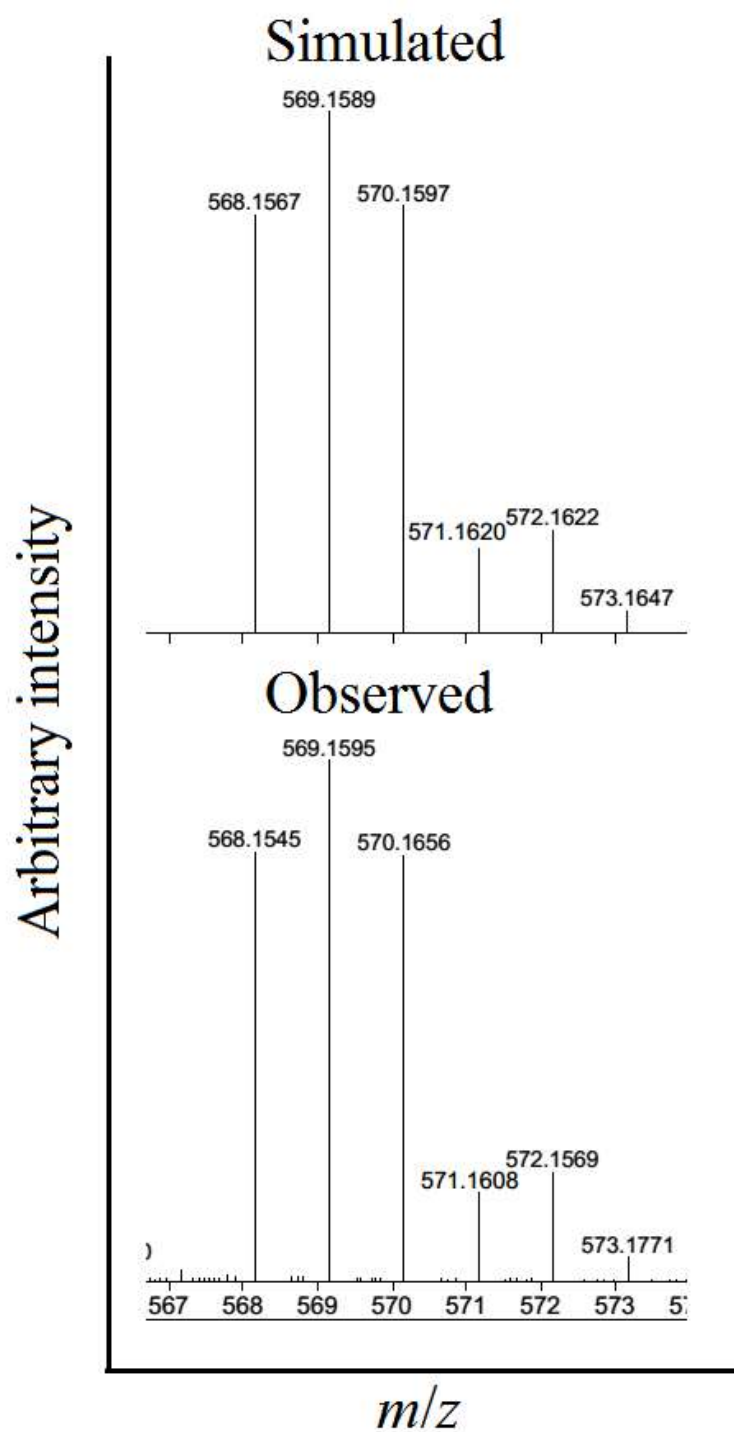


Fig. S23 Observed and simulated isotopic pattern of [**1e** (Scheme 4)] found in ESI-MS.

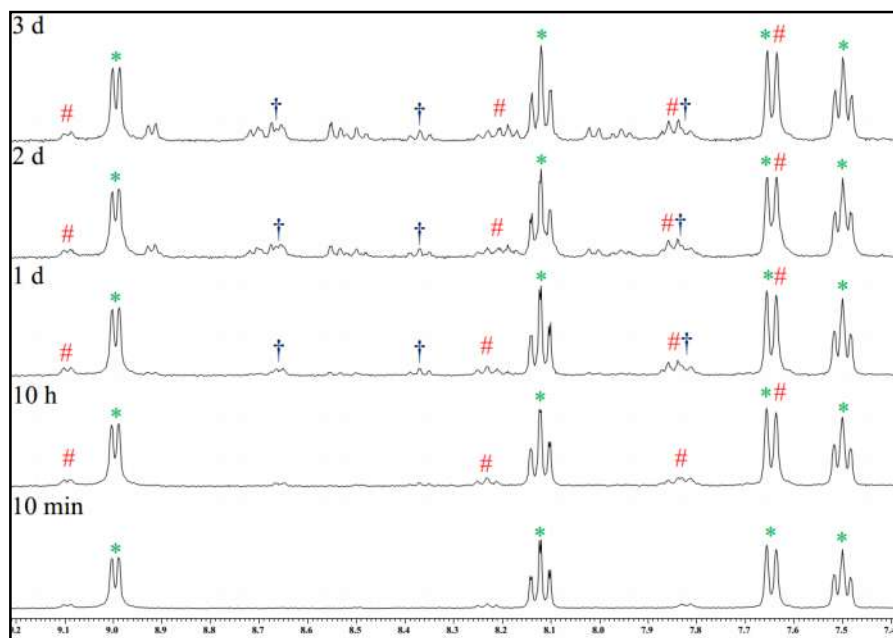


Fig. S24 Stack plot of aromatic region during the stability kinetics study of complex **2** in 20% PBS (pD 7.4, prepared in D₂O) – DMSO-*d*₆ mixture by ¹H NMR, where *, # and † indicate the signals of intact complex **2**, hydrolyzed complex **2a** and aziridinium ion **2b** respectively.

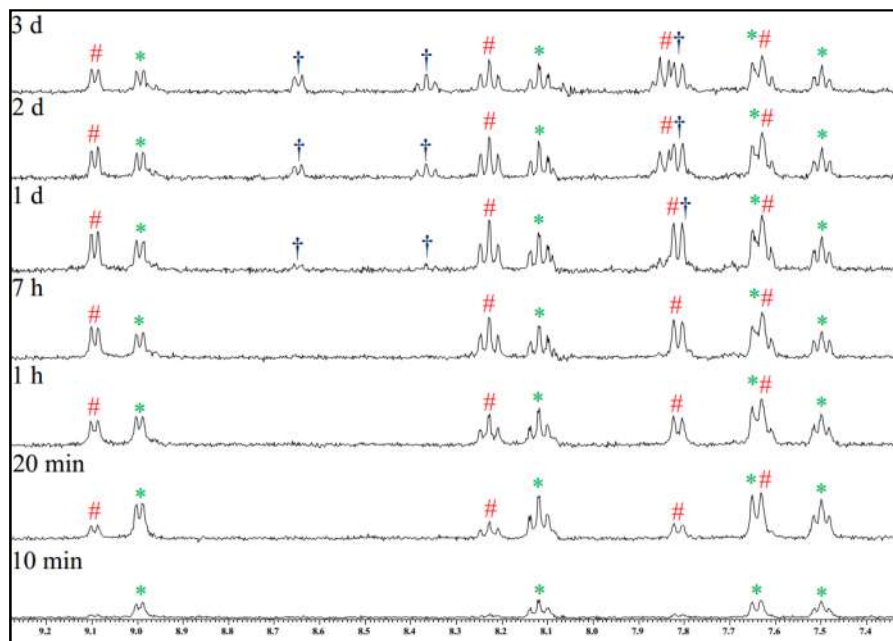


Fig. S25 Stack plot of aromatic region during the stability kinetics study of complex **2** in 20% water – DMSO-*d*₆ mixture by ¹H NMR, where where *, # and † indicate the signals of intact complex **2**, hydrolyzed complex **2a** and aziridinium ion **2b** respectively.

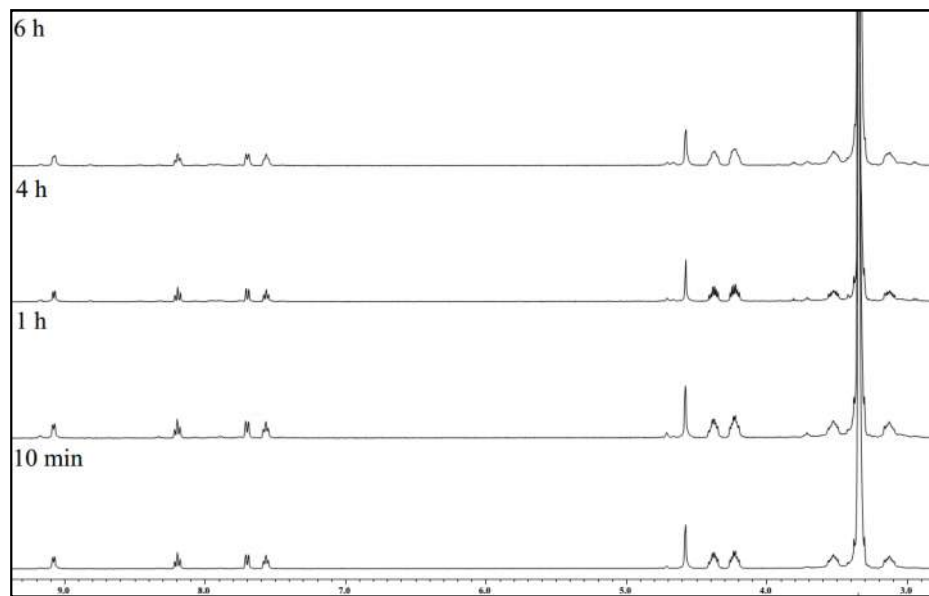


Fig. S26 Stack plot of stability kinetics study of complex **2** in DMSO- d_6 by ^1H NMR.

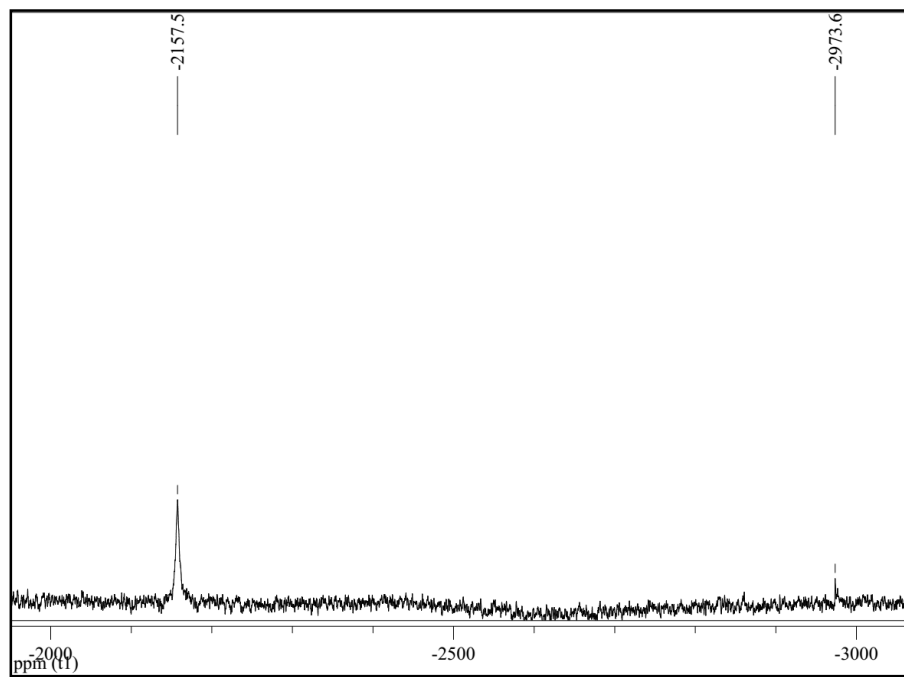


Fig. S27 ^{195}Pt NMR of complex **2** in DMSO- d_6 after 8 h where peak at -2157.5 and -2973.6 ppm represent the chemical shift of **2** and DMSO bound complex **2** respectively.

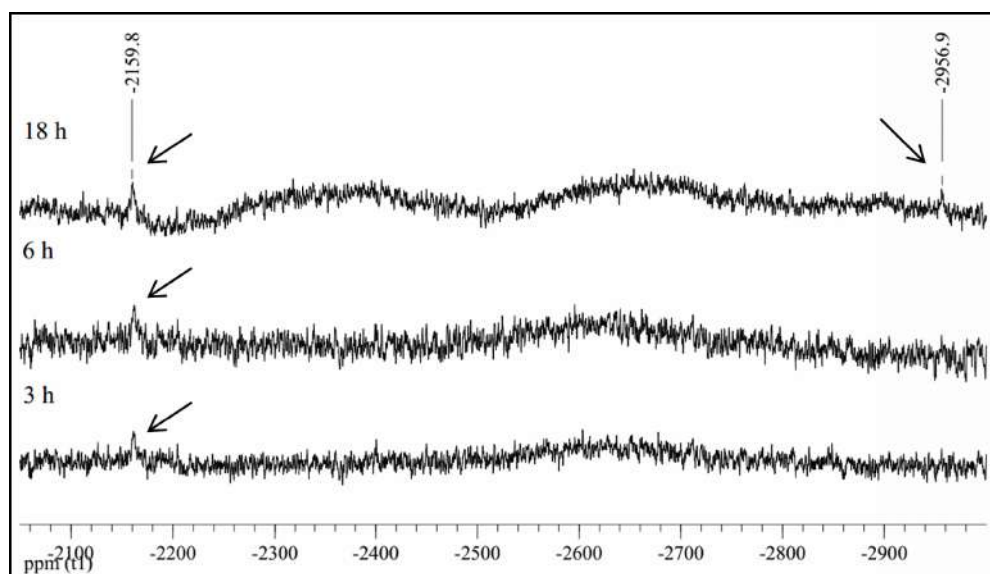


Fig. S28 Stack plot of stability kinetics study of **2** (6 mM) in 40% DMEM-DMSO- d_6 by ^{195}Pt NMR. The peak at -2159.8 ppm is for intact complex **2** and peak at -2956.9 may signify S-bonded **2**. During experimentation some amount of the native complex precipitated.

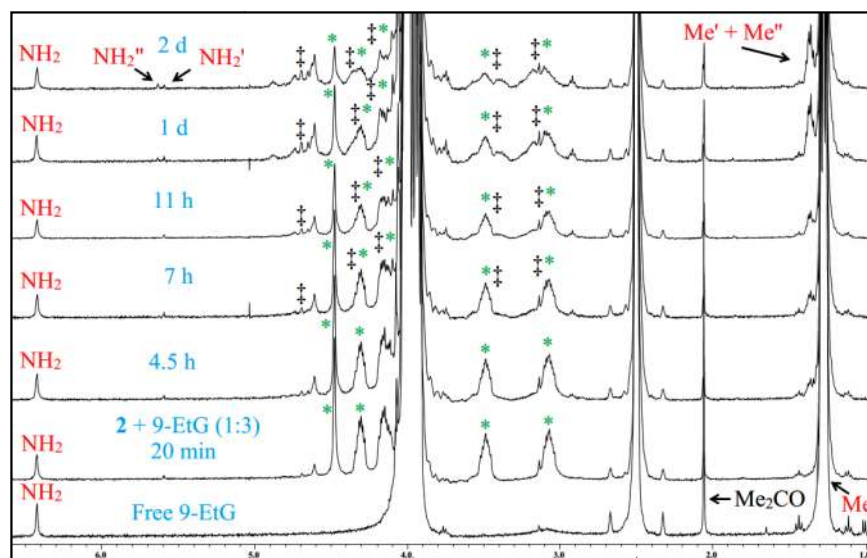


Fig. S29 Stack plot of aliphatic region during the binding kinetics study of **2** with 9-EtG (1:3) in 20% PBS (pD 7.4, prepared in D_2O) – DMSO- d_6 by ^1H NMR, where * and ‡ indicate the signals of intact complex **2** and 9-EtG bound complexes **2d** & **2e** respectively. NH_2 of free 9-EtG is shifted upfield to NH_2' & NH_2'' of 9-EtG bound complexes **2d** & **2e** respectively. **Me** of free 9-EtG is shifted downfield to **Me'** & **Me''** of 9-EtG bound complexes **2d** & **2e** respectively.

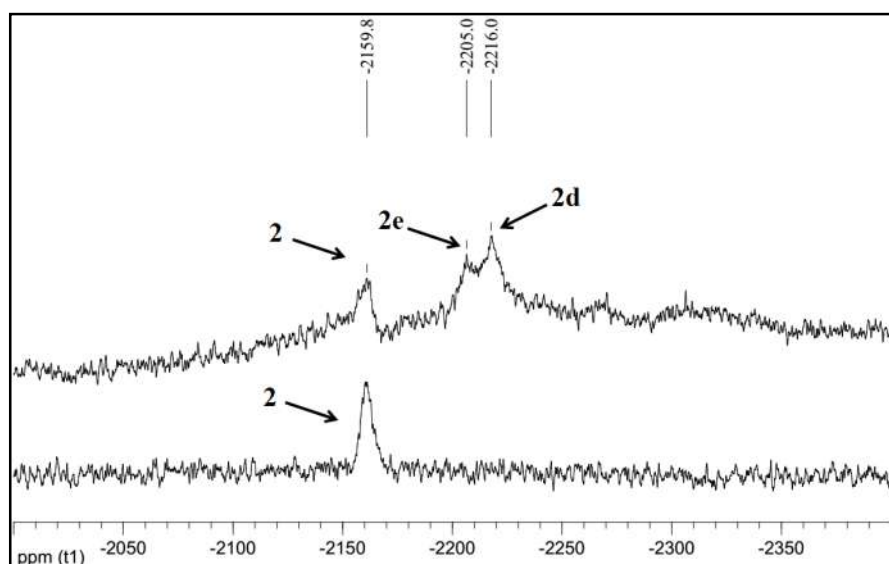


Fig. S30 Stack plot of binding kinetics study of **2** with 9-EtG (1:3) in 20% PBS (pD 7.4, prepared in D₂O) – DMSO-*d*₆ by ¹⁹⁵Pt NMR. The data taken after 2 h shows no binding of 9-EtG with **2**. After 24 h complex **2** signal at –2159.8 ppm diminished and two closely spaced signals of 9-EtG bound complexes **2d** & **2e** at –2216.0 & –2205.0 ppm respectively appear.

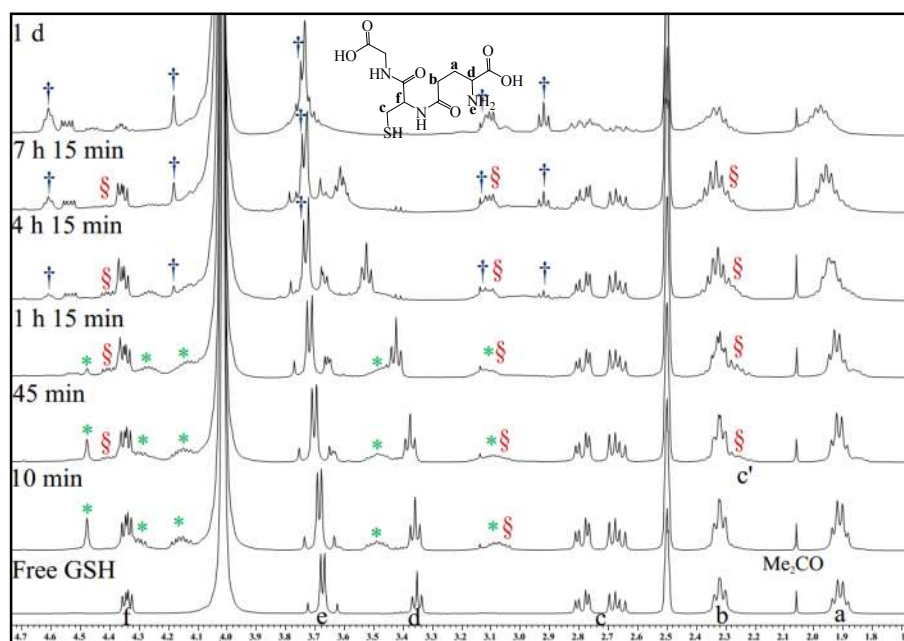


Fig. S31 Stack plot of aliphatic region during the binding kinetics study of **2** with GSH in 20% PBS (pD 7.4, prepared in D₂O) – DMSO-*d*₆ by ¹H NMR, where *, § and † indicate the signals of intact complex **2**, GSH bound complex **2c** and aziridinium ion **2b** respectively.

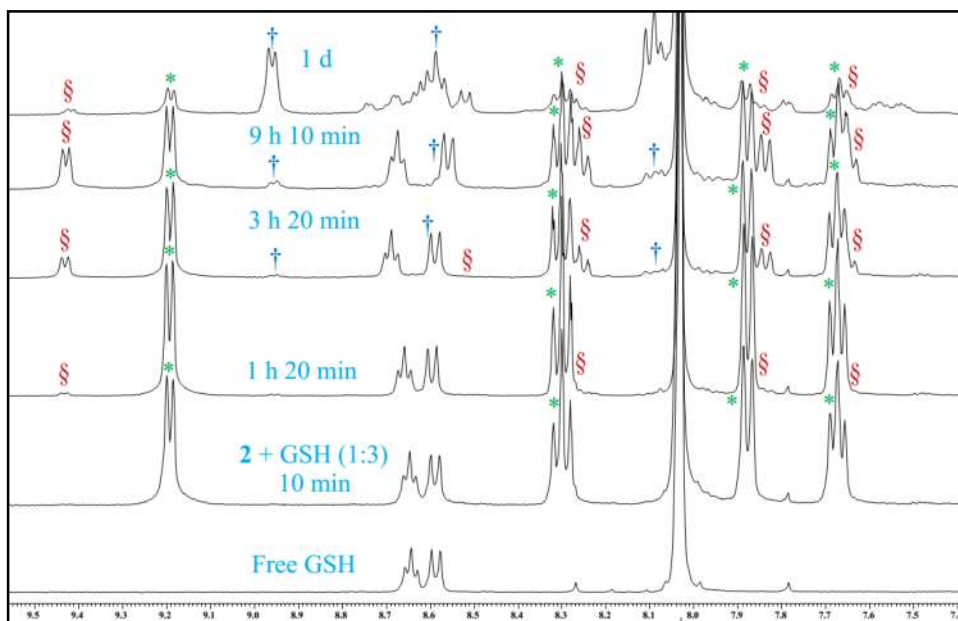


Fig. S32 Stack plot of aromatic region during the binding kinetics study of **2** with GSH in 20% PBS (pD 7.4, prepared in D₂O) – DMF-*d*₇ by ¹H NMR, where *, § and † indicate the signals of intact complex **2**, GSH bound complex **2c** and aziridinium ion **2b** respectively.

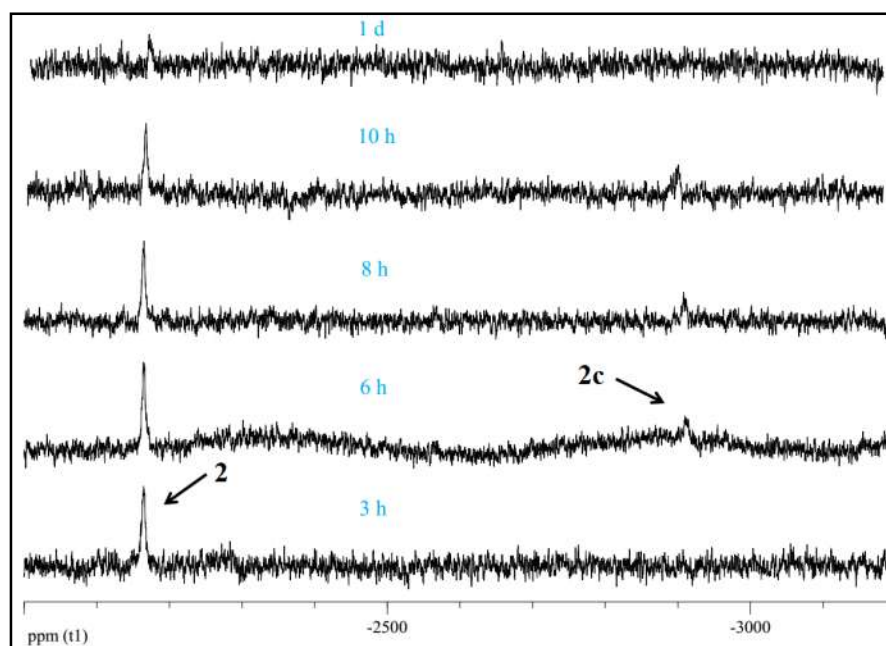


Fig. S33 Stack plot of binding kinetics study of **2** with GSH (1:3) in 20% PBS (pD 7.4, prepared in D₂O) – DMF-*d*₇ by ¹⁹⁵Pt NMR. After 6 h complex signal GSH bound complex **2c** at –2910.9 ppm appears along with initial signal of complex **2** at –2164.6 ppm. After a day the ¹⁹⁵Pt signal of **2c** vanishes with very small amount of unreacted complex **2** signal.

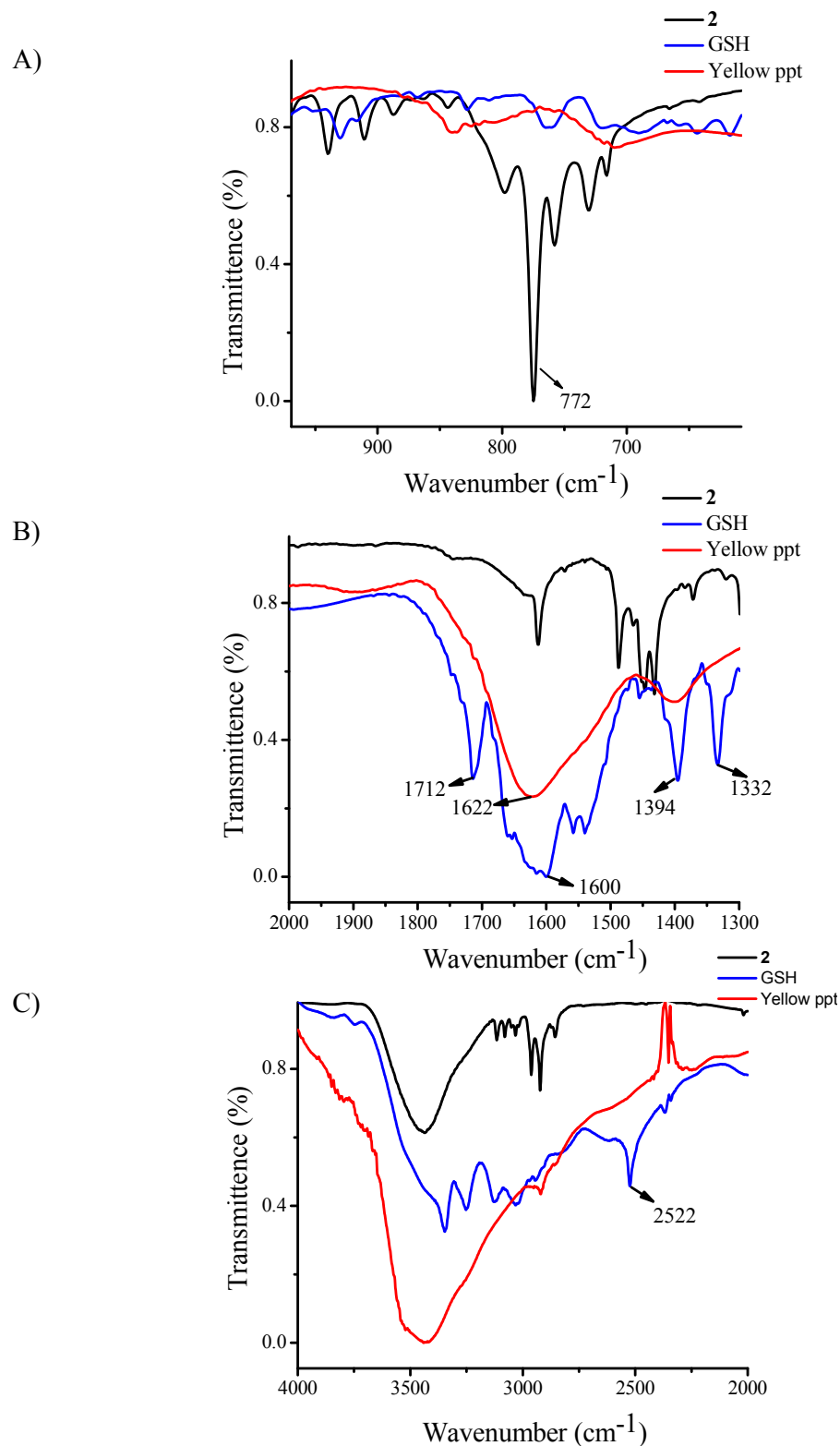
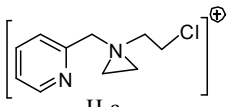


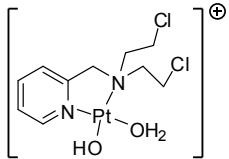
Fig. S34 Stack plot of IR spectra of **2**, GSH and yellow ppt found in the reaction of **2** with GSH (1:3) in 20% PBS (pD 7.4, prepared in D_2O) – $\text{DMF-}d_7$. A) Sharp band of C–Cl stretching frequency 772 cm^{-1} of **2** vanished in yellow ppt. B) Carbonyl stretching band of GSH and yellow ppt. C) S–H stretching band at 2522 cm^{-1} in GSH vanished in yellow ppt and a broad band at $3550\text{--}2700\text{ cm}^{-1}$ for polymeric nature of yellow ppt.

Table S3 Species found in ESI-MS during the stability/binding kinetics studies of **2** by ^1H NMR. The drawings of the respective species are given below the tabulated data

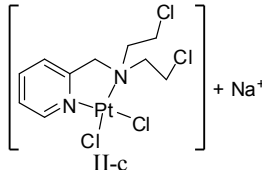
Species no.	m/z_{calc}	Experiments			
		2 in 20% PBS in $\text{DMSO-}d_6$	2 in 20% H_2O in $\text{DMSO-}d_6$	2 + 9-EtG (1:3) in 20% PBS in $\text{DMSO-}d_6$	2 + GSH (1:3) in 20% PBS in $\text{DMSO-}d_6$
		m/z_{obs}			
II-a	197.0845	197.0846	197.0832	-	197.0832
II-b	463.0297	462.9756	462.9728	462.9782	462.9832
II-c	520.9429	520.9438	520.9869	520.9448	520.9427
II-d	540.9330	540.9924	540.9805	540.9927	-
II-e	606.0896	-	-	606.0881	-
II-f	642.0657	-	-	642.0645	-
II-g	179.1184	-	-	-	179.0498
II-h	233.0612	-	-	-	233.0599
II-i	308.0916	-	-	-	308.0837
II-j	330.0736	-	-	-	330.0706
II-k	352.0555	-	-	-	352.0511
II-l	374.0375	-	-	-	374.0371
II-m	734.0927	-	-	-	734.1046
II-n	770.0688	-	-	-	770.0684
II-o	792.0508	-	-	-	792.0432
II-p	814.0327	-	-	-	814.0229
II-q	836.0146	-	-	-	836.0093
I-b	427.0539	427.0096	427.0059	427.0033	-
I-f	180.0885	-	180.0859	180.0859	-
I-g	202.0705	-	211.0636	211.0636	-
I-h	218.0444	-	218.0458	218.0458	-
I-i	381.1512	-	-	381.1545	-
I-l	739.3126	-	-	739.3130	-



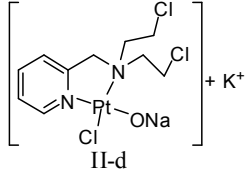
II-a



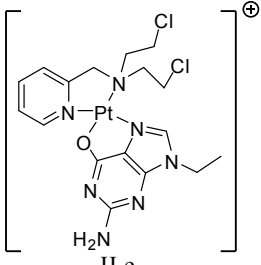
II-b



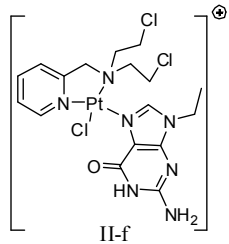
II-c



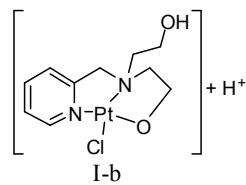
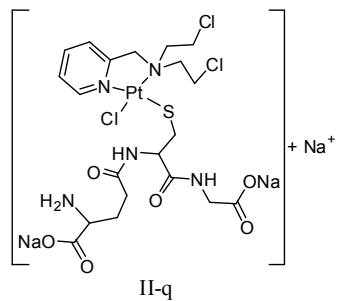
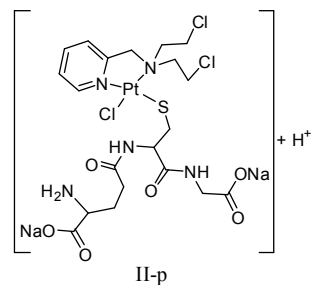
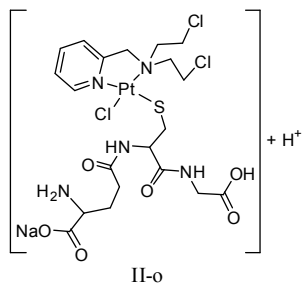
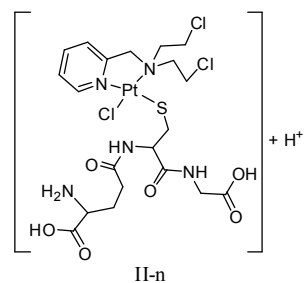
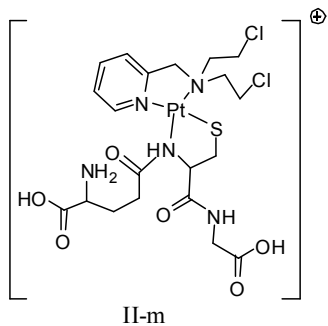
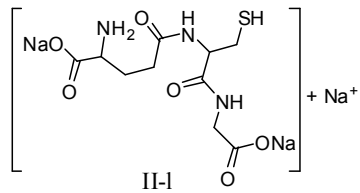
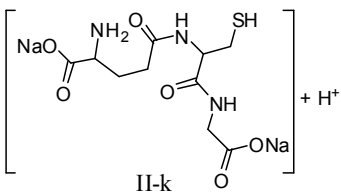
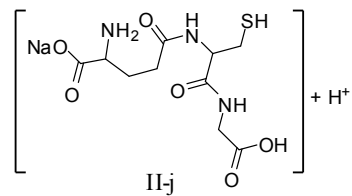
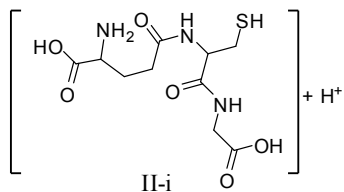
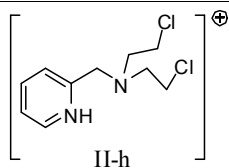
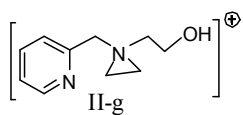
II-d



II-e



II-f



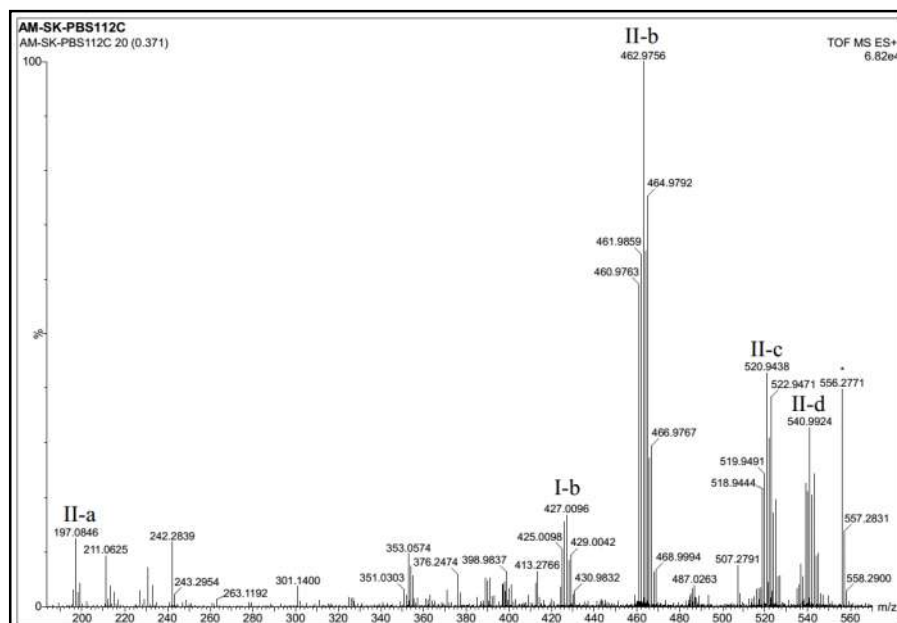
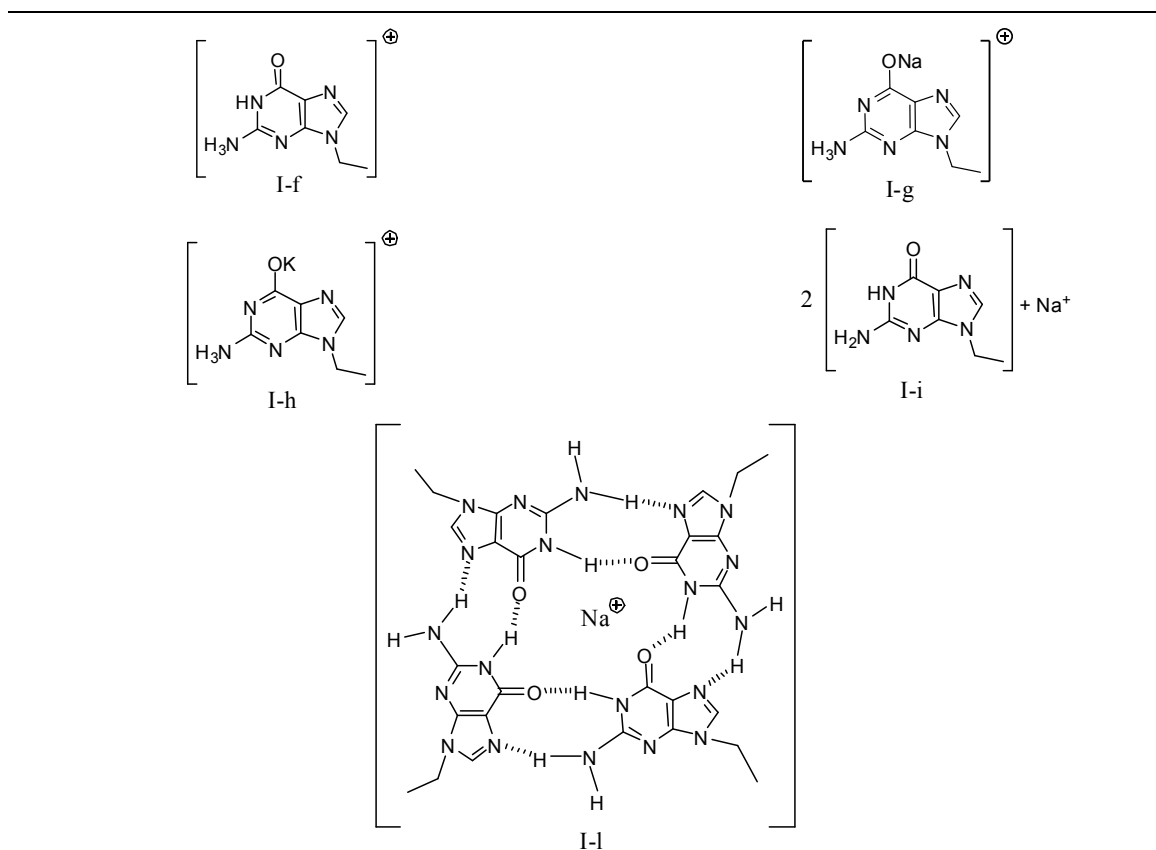


Fig. S35 ESI-MS speciation recorded during monitoring of stability kinetics of the complex **2** by ^1H NMR after 1 d in 20% PBS (pD 7.4, prepared in D_2O) – $\text{DMSO-}d_6$ mixture.

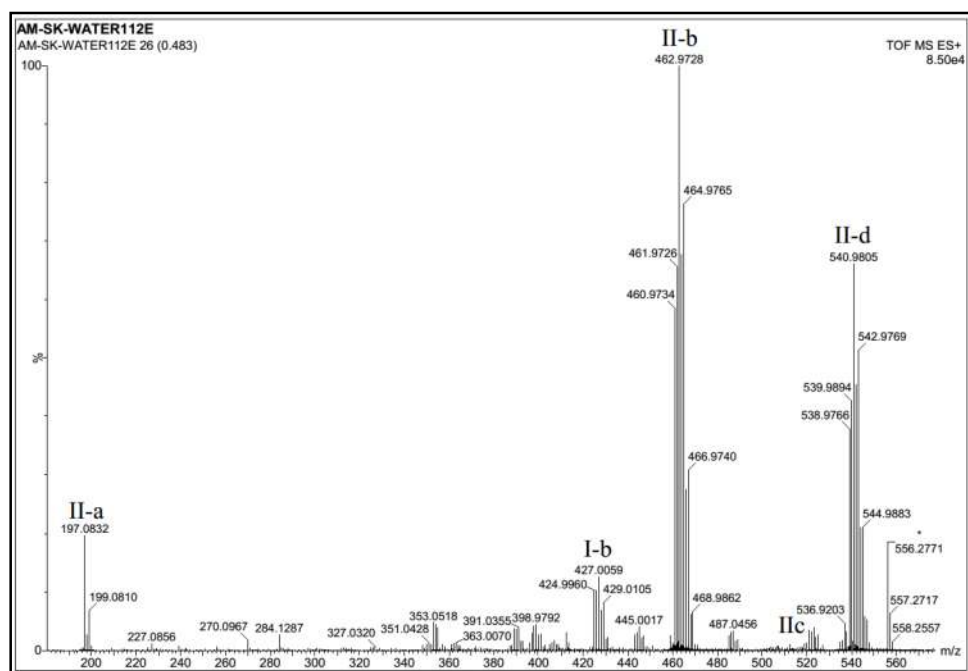


Fig. S36 ESI MS speciation recorded during monitoring of stability kinetics of the complex **2** by ^1H NMR after 3 d in 20% water – $\text{DMSO}-d_6$ mixture.

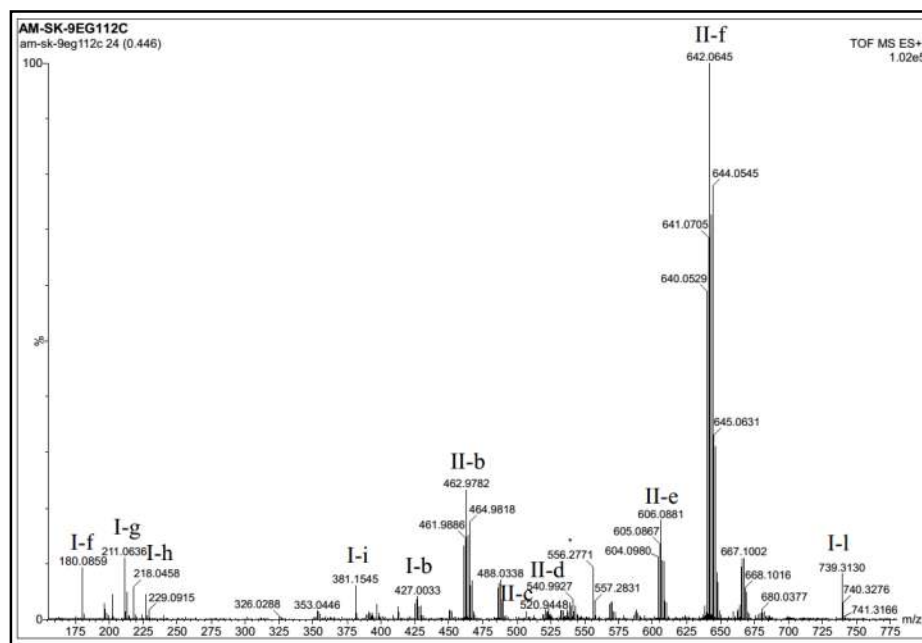


Fig. S37 ESI-MS speciation recorded during monitoring of the 9-EtG binding kinetics with complex **2** by ^1H NMR after 2 d in 20% PBS (pD 7.4, prepared in D_2O) – $\text{DMSO}-d_6$ mixture.

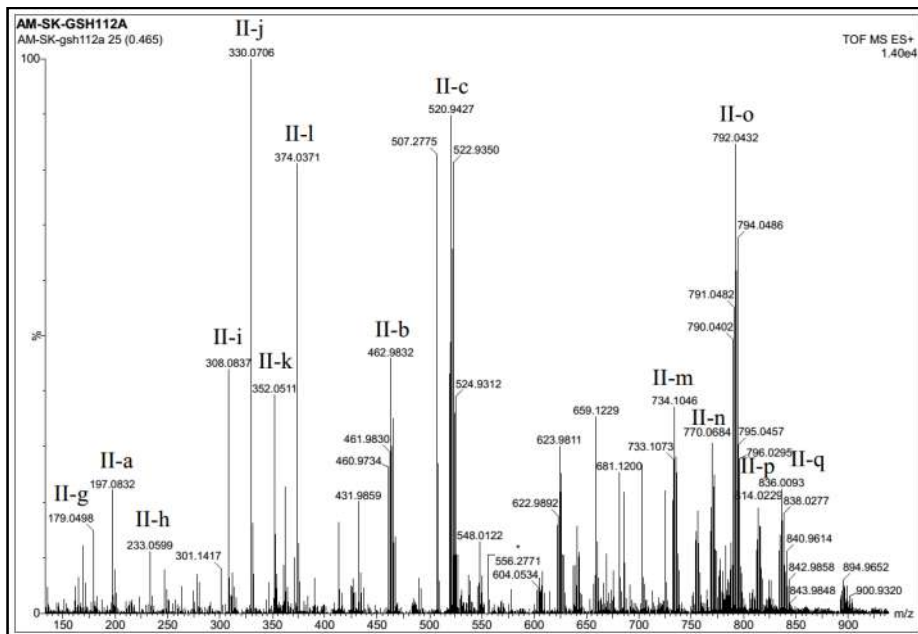


Fig. S38 ESI-MS speciation recorded during monitoring of the GSH binding kinetics with complex **2** by ^1H NMR after 2 h in 20% PBS (pD 7.4, prepared in D_2O) – $\text{DMSO-}d_6$ mixture.

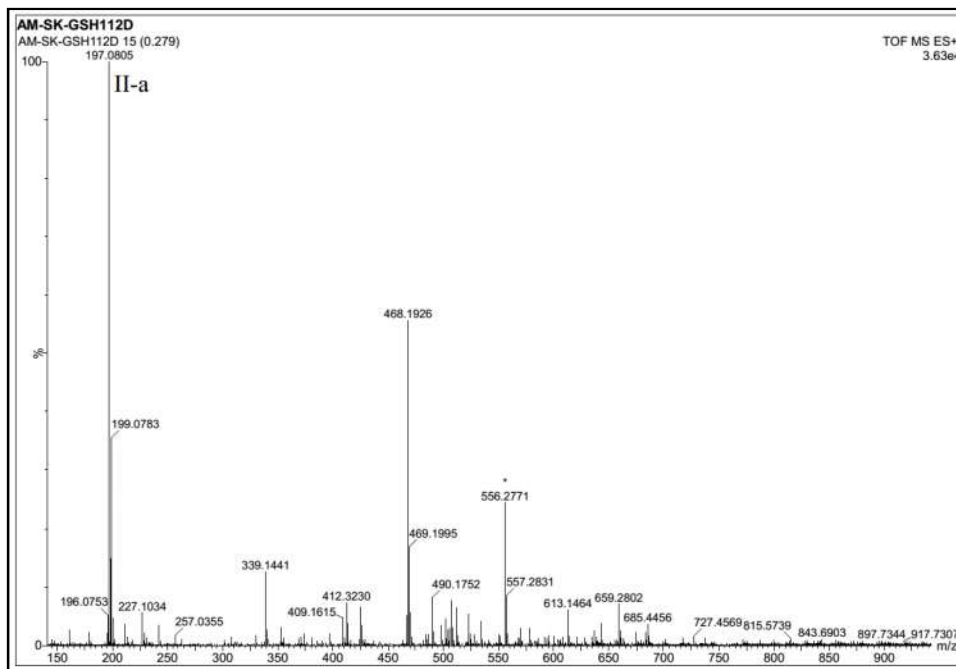


Fig. S39 ESI-MS speciation recorded during monitoring of the GSH binding kinetics with complex **2** by ^1H NMR after 1 d in 20% PBS (pD 7.4, prepared in D_2O) – $\text{DMSO-}d_6$ mixture.

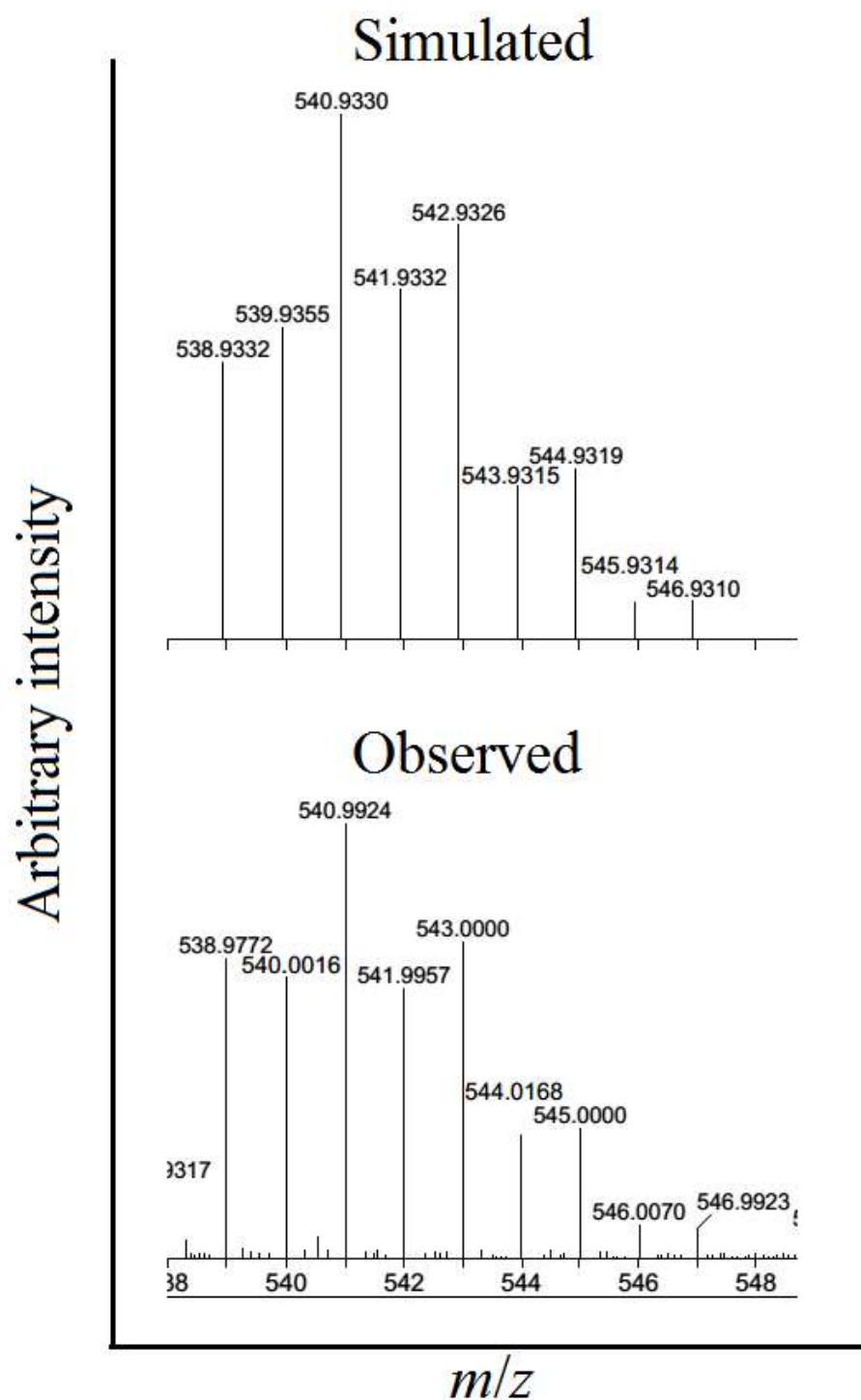


Fig. S40 Observed and simulated isotopic pattern of [**2a** (Scheme 5) – 2H⁺ + Na⁺ + K⁺] found in ESI-MS.

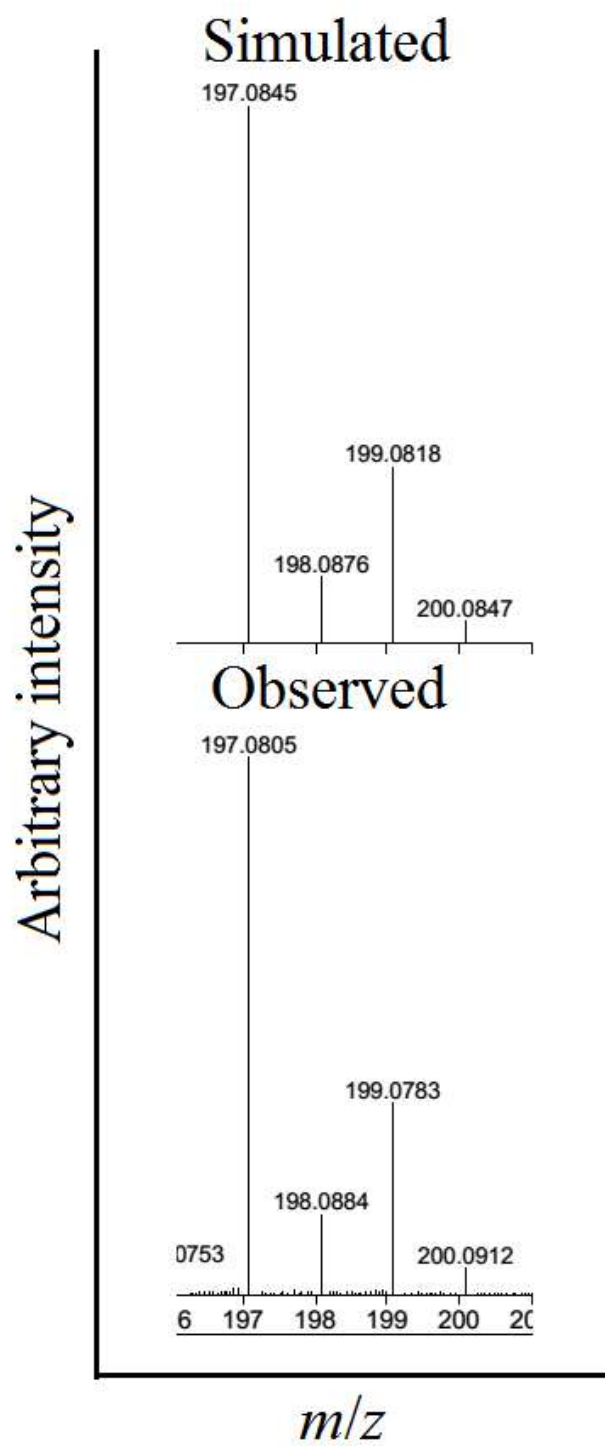


Fig. S41 Observed and simulated isotopic pattern of [**2b** (Scheme 5)] found in ESI-MS.

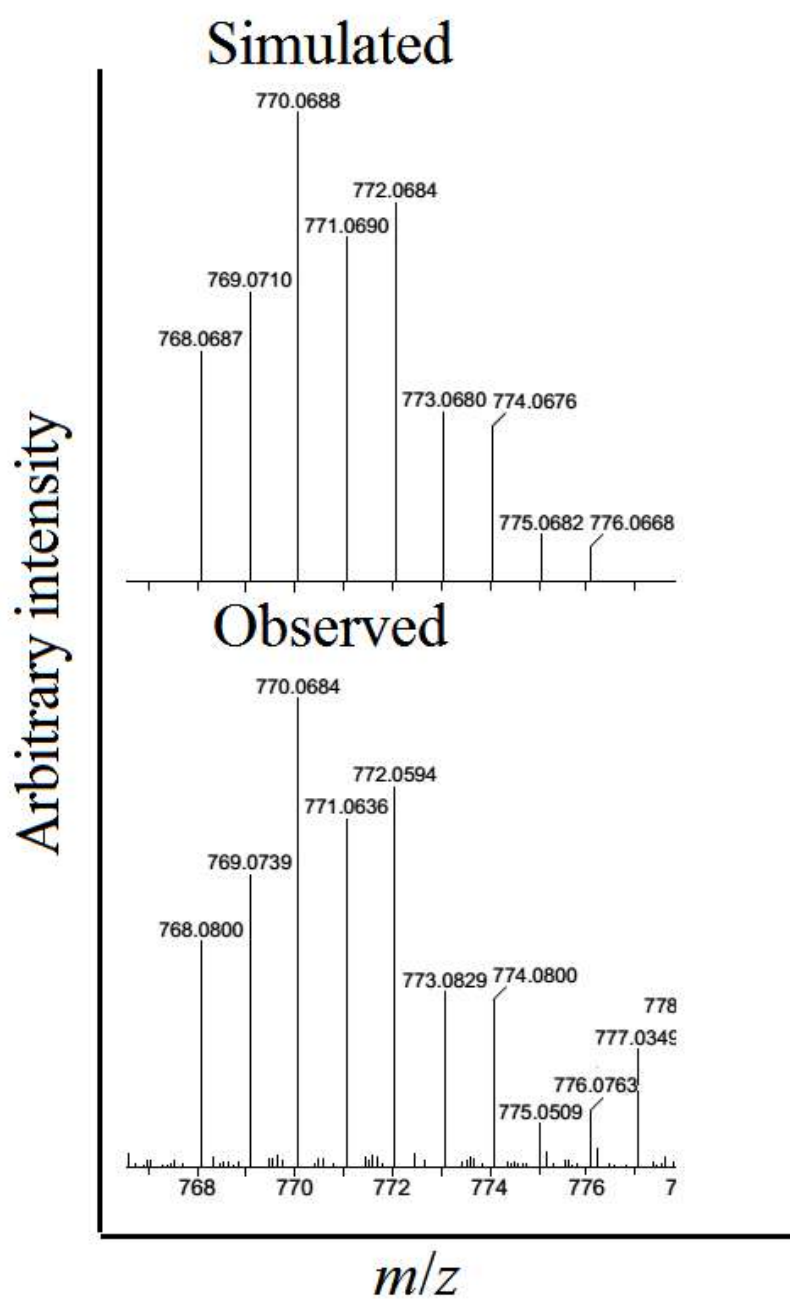


Fig. S42 Observed and simulated isotopic pattern of [**2c** (Scheme 5)] found in ESI-MS.

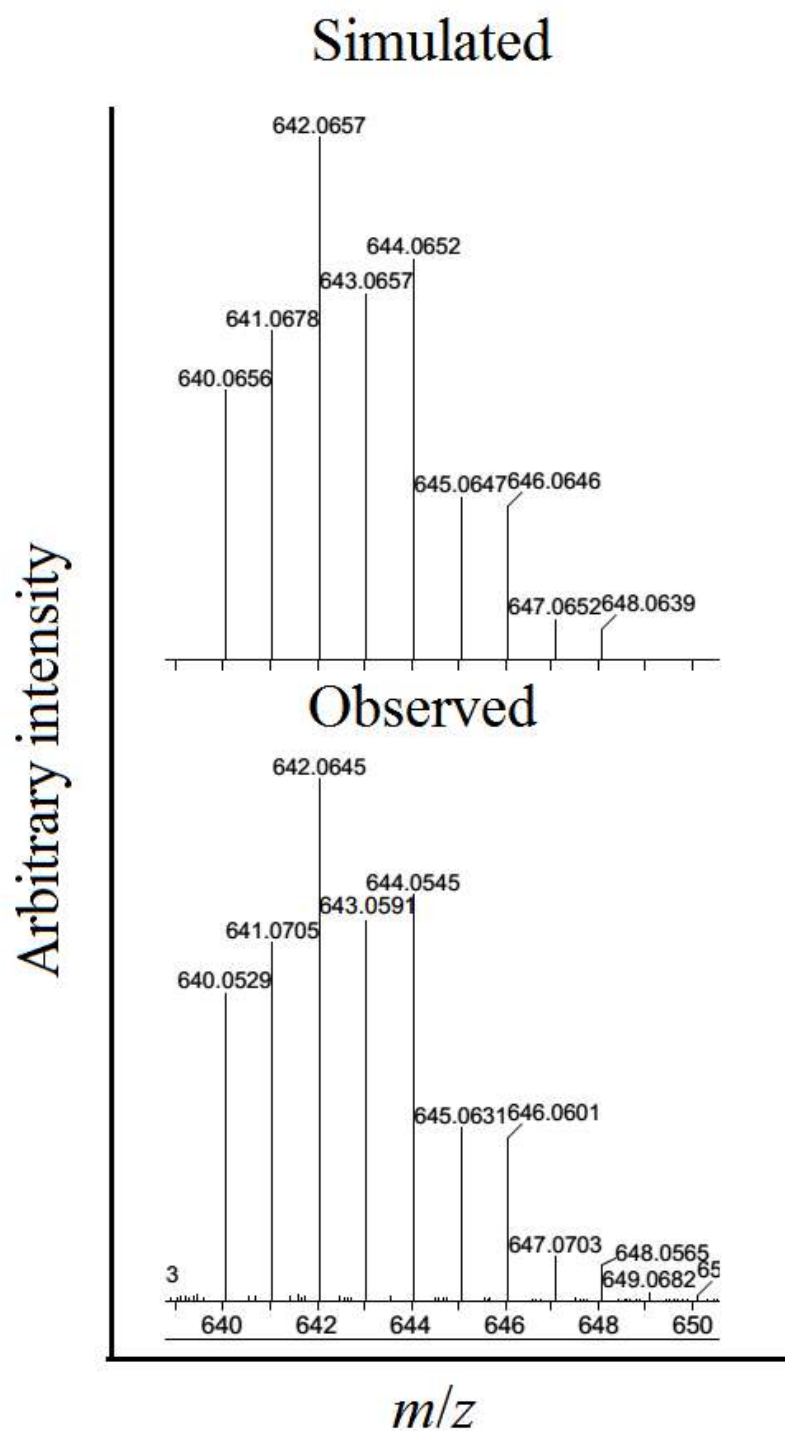


Fig. S43 Observed and simulated isotopic pattern of [**2d** (Scheme 5)] found in ESI-MS.

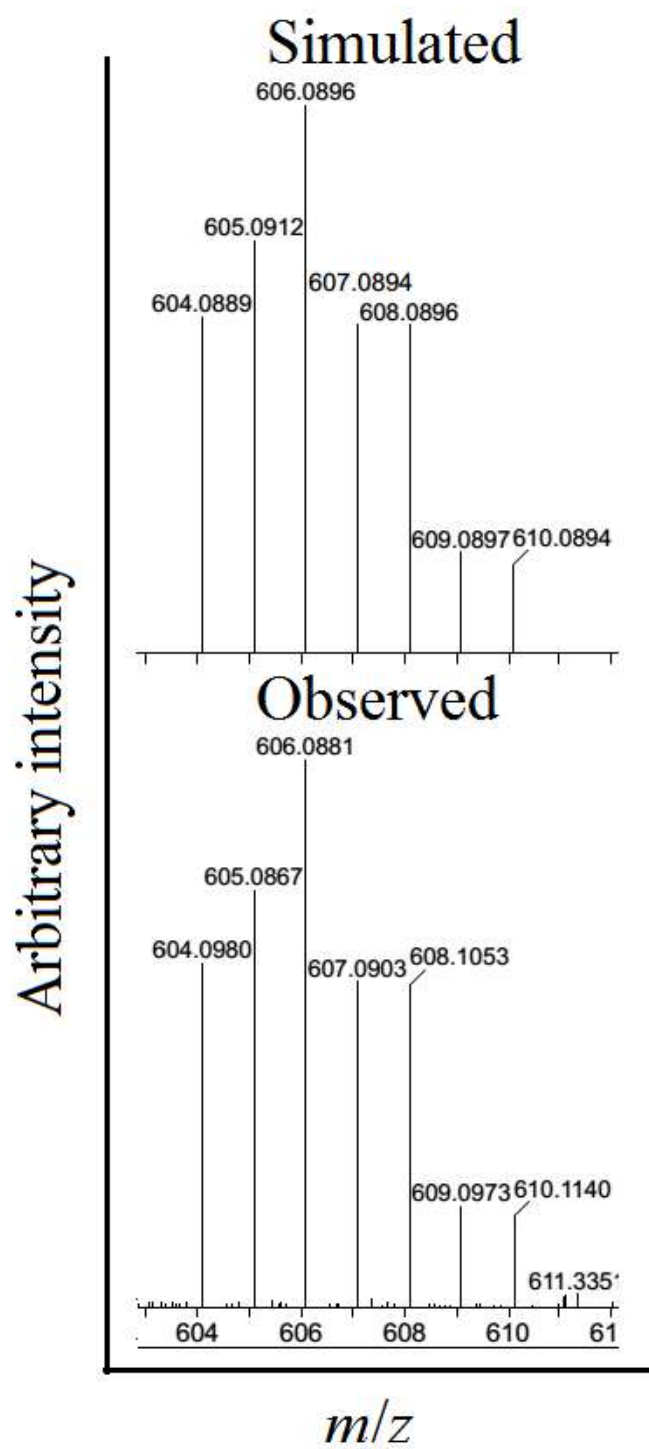


Fig. S44 Observed and simulated isotopic pattern of [**2e** (Scheme 5)] found in ESI-MS.

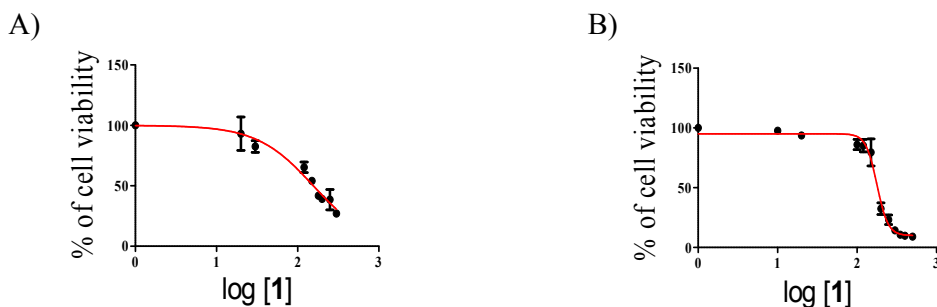


Fig. S45 Plots of cell viability (%) vs. log of μM concentrations of **1** against A) MCF-7 and B) HeLa WT cell lines after incubation for 48 h determined from MTT assays under normoxic condition. The plots provided are for one independent experiment out of the three independent experiments.

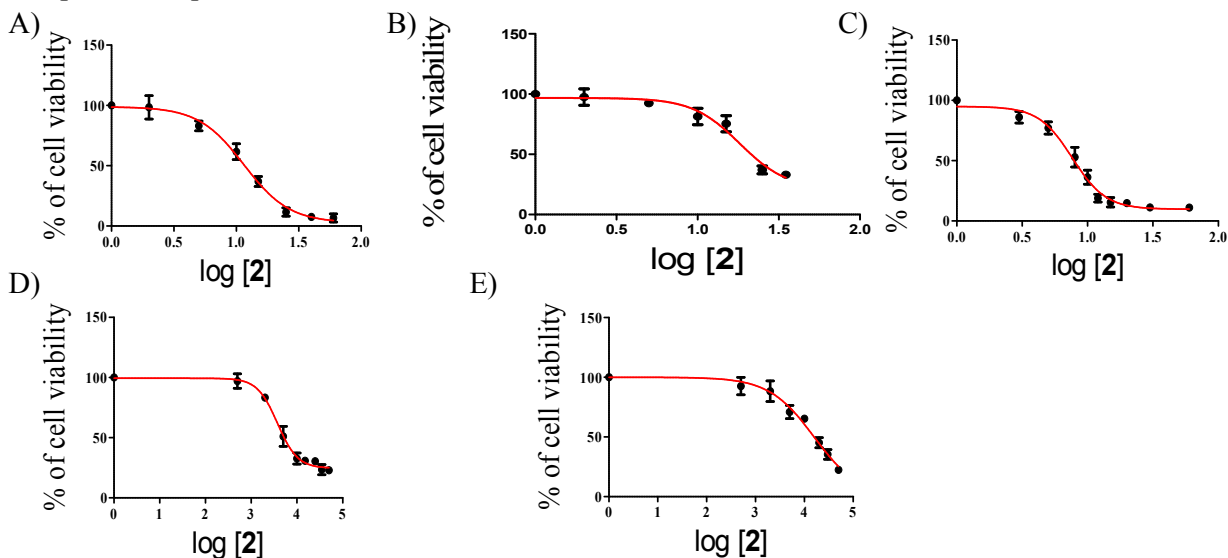


Fig. S46 Plots of cell viability (%) vs. log of μM concentrations of **2** against A) MCF-7, B) A549, C) HeLa WT, D) MIA PaCa2 and E) HEK293 cell lines after incubation for 48 h determined from MTT assays under normoxic condition. The plots provided are for one independent experiment out of the three independent experiments.

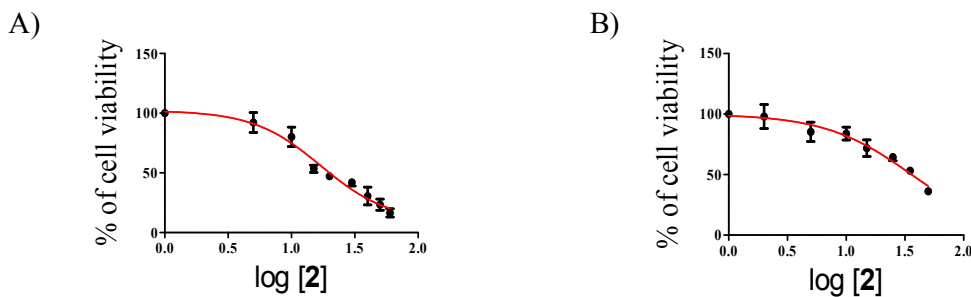


Fig. S47 Plots of cell viability (%) vs. log of μM concentrations of **2** against A) MCF-7 and B) A549 cell lines after incubation for 48 h determined from MTT assays under normoxic condition in presence of 250 μM and 400 μM GSH respectively. The plots provided are for one independent experiment out of the three independent experiments.

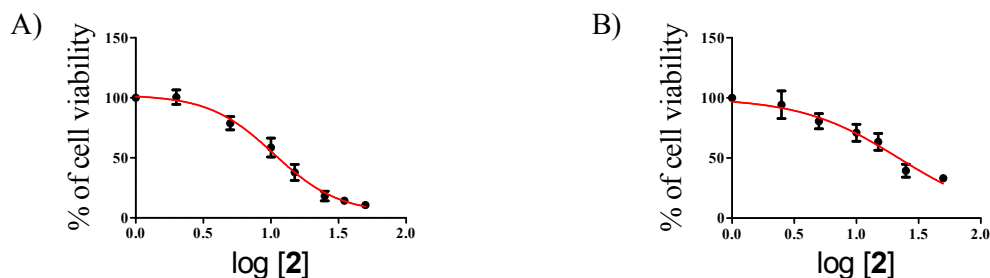


Fig. S48 Plots of cell viability (%) vs. log of μM concentrations of **2** against A) MCF-7 and B) A549 cell lines after incubation for 48 h determined from MTT assays under hypoxic condition. The plots provided are for one independent experiment out of the three independent experiments.

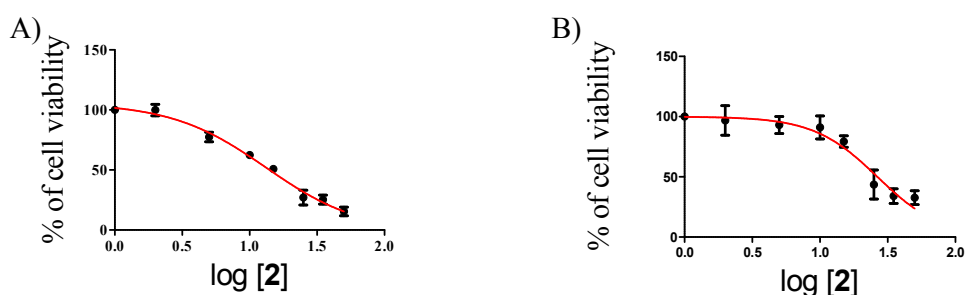


Fig. S49 Plots of cell viability (%) vs. log of μM concentrations of **2** against A) MCF-7 and B) A549 cell lines after incubation for 48 h determined from MTT assays under hypoxic condition in presence of 250 μM and 400 μM GSH respectively. The plots provided are for one independent experiment out of the three independent experiments.

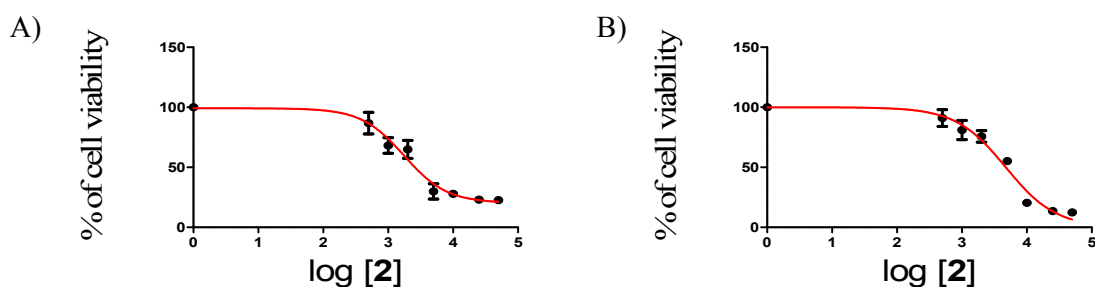


Fig. S50 Plots of cell viability (%) vs. log of μM concentrations of **2** against A) MIA PaCa2 cell line after incubation for 48 h determine from MTT assays under hypoxic condition and B) MIA PaCa2 cell lines after incubation for 48 h under hypoxic condition in presence of 100 μM GSH determined from MTT assays. The plots provided are for one independent experiment out of the three independent experiments.

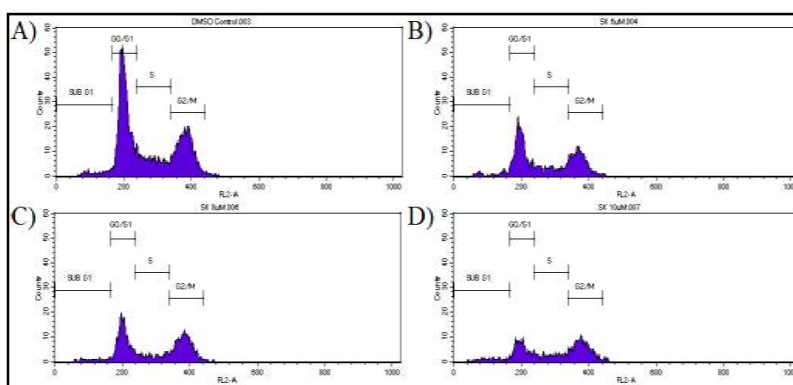


Fig. S51 Cell cycle arrest of MCF-7 treated with **2** for 24 h. (A) DMSO control, (B) 6 μ M, (C) 8 μ M and D) 10 μ M of **2** treated cells. The figure represents one independent experiment.

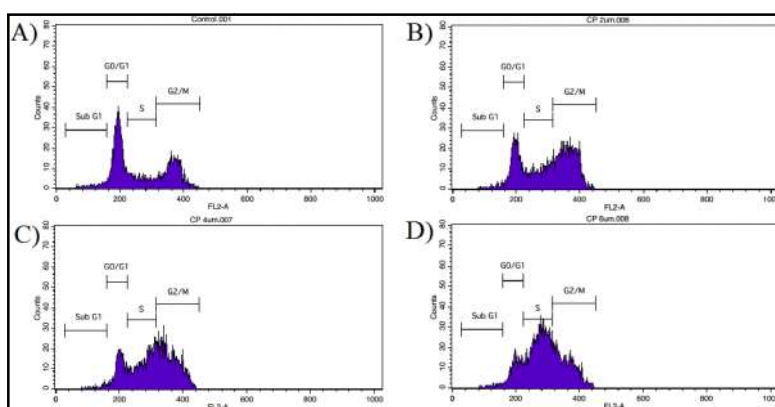


Fig. S52 Cell cycle arrest of MCF-7 treated with cisplatin for 24 h. (A) DMSO control, (B) 2 μ M, (C) 4 μ M and D) 6 μ M of cisplatin treated cells. The figure represents one independent experiment.

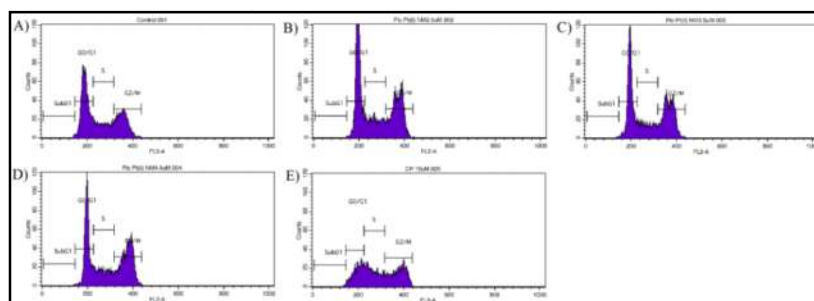


Fig. S53 Cell cycle arrest of MIA PaCa2 treated with **2** and cisplatin respectively for 24 h. (A) DMSO control, (B) 2.5 μ M, (C) 3.5 μ M and D) 4.5 μ M of **2** and 15 μ M of cisplatin treated cells. The figure represents one independent experiment.

Table S4 Cell cycle analysis of MCF-7 cells treated with **2**^a

	Sub G1	G0/G1	S	G2/M
DMSO control ^b	3.9	43.9	22.4	29.8
2 , 6 μM ^b	5.6	35.4	20.4	38.6
2 , 8 μM ^b	6.5	30.4	19.3	43.8
2 , 10 μM ^b	8.1	24.7	22.1	45.1

^aCells were treated with the complex for 24 h. Cell populations were expressed as the percentage of cells in each phase. ^bThe data represents the average of two independent experiments.

Table S5 Cell cycle analysis of MCF-7 cells treated with cisplatin^a

	Sub G1	G0/G1	S	G2/M
DMSO control ^b	1.2	50.9	17.4	30.5
Cisplatin, 2 μM ^b	1.2	24.5	26.6	47.7
Cisplatin, 4 μM ^b	1.1	18.9	44.2	35.8
Cisplatin, 6 μM ^b	1.0	19.2	58.7	21.1

^aCells were treated with the complex for 24 h. Cell populations were expressed as the percentage of cells in each phase. ^bThe data represents the average of two independent experiments.

Table S6 Cell cycle analysis of MIA PaCa2 cells treated with **2** and cisplatin^a

	Sub G1	G0/G1	S	G2/M
DMSO control ^b	1.0	47.6	21.8	29.6
2 , 2.5 μM ^b	1.0	44.3	19.3	35.4
2 , 3.5 μM ^b	1.0	41.2	18.5	39.3
2 , 4.5 μM ^b	1.0	35.9	20.0	43.1
Cisplatin, 15 μM ^b	1.0	27.1	32.9	39.0

^aCells were treated with the complex for 24 h. Cell populations were expressed as the percentage of cells in each phase. ^bThe data represents the average of two independent experiments.